Article

A Redox-Driven Multicomponent Molecular Shuttle

Sourav Saha, Amar H. Flood, J. Fraser Stoddart, Stefania Impellizzeri, Serena Silvi, Margherita Venturi, and Alberto Credi

J. Am. Chem. Soc., **2007**, 129 (40), 12159-12171• DOI: 10.1021/ja0724590 • Publication Date (Web): 19 September 2007

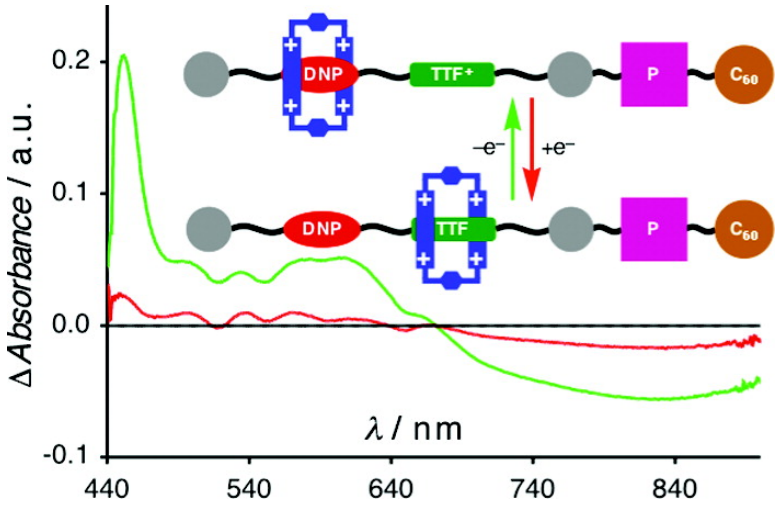

More About This Article

Additional resources and features associated with this article are available within the HTML version:

- Supporting Information
- Links to the 19 articles that cite this article, as of the time of this article download
- Access to high resolution figures
- Links to articles and content related to this article
- Copyright permission to reproduce figures and/or text from this article

View the Full Text HTML

J|A|C|S
ARTICLES
Published on Web 09/19/2007

A Redox-Driven Multicomponent Molecular Shuttle

Sourav Saha,[†] Amar H. Flood,[‡] J. Fraser Stoddart,*[,†] Stefania Impellizzeri,[§] Serena Silvi,[§] Margherita Venturi,[§] and Alberto Credi*[,§]

Contribution from the California NanoSystems Institute and the Department of Chemistry and Biochemistry, University of California, Los Angeles, California 90095, Department of Chemistry, Indiana University, Bloomington, Indiana 47405, and Dipartimento di Chimica "G. Ciamician", Università di Bologna, via Selmi 2, 40126 Bologna, Italy

Received April 9, 2007; E-mail: stoddart@chem.ucla.edu; alberto.credi@unibo.it

Abstract: A multicomponent [2]rotaxane designed to operate as a molecular shuttle driven by light energy has been constructed, and its properties have been investigated. The system is composed of (1) a light-fueled power station, capable of using the photon energy to create a charge-separated state, and (2) a mechanical switch, capable of utilizing such a photochemically generated driving force to bring about controllable molecular shuttling motions. The light-fueled power station is, in turn, a dyad comprising (i) a π-electron-accepting fullerene (C_{60}) component and (ii) a light-harvesting porphyrin (P) unit which acts as an electron donor in the excited state. The mechanical switch is a redox-active bistable [2]rotaxane moiety that consists of (i) a tetrathiafulvalene (TTF) unit as an efficient π-electron-donor station, (ii) a dioxynaphthalene (DNP) unit as a second π-electron-rich station, and (iii) a tetracationic cyclobis(paraquat-*p*-phenylene) ($CBPQT^{4+}$) π-electron-acceptor cyclophane, which encapsulates the better π-electron-donating TTF station. Diethylene glycol spacers were conveniently introduced between the electroactive components in the dumbbell-shaped thread to facilitate the template-directed synthesis of the [2]rotaxane. A modular synthetic approach was undertaken for the overall synthesis of this multicomponent bistable [2]rotaxane, beginning with the syntheses of the P−C_{60} dyad unit and the two-station TTF−DNP-based [2]rotaxane separately, using conventional synthetic methodologies. These two components were finally stitched together by an esterification to afford the target rotaxane. Its structure was characterized by ^{1}H NMR spectroscopy and mass spectrometry as well as by UV−vis−NIR absorption spectroscopy and voltammetry. The observations reflect remarkable electronic interactions between the various units, pointing to the existence of folded conformations in solution. The redox-driven shuttling process of the $CBPQT^{4+}$ ring between the two competitive electron-rich recognition units, namely, TTF and DNP, was investigated by electrochemistry and spectroelectrochemistry as a means to verify its operational behavior prior to the photophysical studies related to light-driven operation. The oxidation process of the TTF unit is dramatically hampered in the rotaxane, thereby reducing the efficiency of the shuttling motion. These results confirm that, as the structural complexity increases, the overall function of the system no longer depends simply on its "primary" structure but also on higher-level effects which are reminiscent of the secondary and tertiary structures of biomolecules.

Introduction

The construction of mechanical machines at the ultimate level of miniaturization, i.e., that of molecules, is a formidable challenge for research in nanoscience and nanotechnology.[1,2] The scientific basis for this idea is rooted in the existence of natural molecular machines[3] that carry out many essential functions in living organisms, including human beings. In fact, these biological nanomachines constitute the premier, proven examples of the utility and feasibility of a nanotechnology based on soft materials.[4]

Just like their macroscopic counterparts, molecular machines need a power supply that can fuel mechanical movements. While macroscopic machines do not move or work until energy is supplied to it for a specific function, machines on the molecular level are in perpetual random (Brownian) motion at ambient temperature.[4b,5] Hence, the energy supplied to molecular

[†] University of California.
[‡] Indiana University.
[§] Università di Bologna.

(1) (a) Balzani, V.; Credi, A.; Venturi, M. *Molecular Devices and Machines − A Journey into the Nano World*; Wiley-VCH: Weinheim, 2003. (b) *Top. Curr. Chem.* **2005**, *262*, 1−227 (Special volume on molecular motors; Kelly, T. R., Ed.).
(2) (a) Balzani, V.; Credi, A.; Raymo, F. M.; Stoddart, J. F. *Angew. Chem., Int. Ed.* **2000**, *39*, 3348−3391. (b) Flood, A. H.; Ramirez, R. J. A.; Deng, W.-Q.; Muller, R. P.; Goddard, W. A.; Stoddart, J. F. *Aust. J. Chem.* **2004**, *57*, 301−322. (c) Kinbara, K.; Aida, T. *Chem. Rev.* **2005**, *105*, 1377−1400. (d) Chatterjee, M. N.; Kay, E. R.; Leigh, D. A. *J. Am. Chem. Soc.* **2006**, *128*, 4058−4073. (e) Tian, H.; Wang, Q. C. *Chem. Soc. Rev.* **2006**, *35*, 361−374. (f) Bonnet, S.; Collin, J.-P.; Koizumi, M.; Mobian, P.; Sauvage, J.-P. *Adv. Mater.* **2006**, *18*, 1239−1250. (g) Browne, W. L.; Feringa, B. L. *Nat. Nanotechnol.* **2006**, *1*, 25−35. (h) Kay, E. R; Leigh, D. A.; Zerbetto, F. *Angew. Chem., Int. Ed.* **2007**, *46*, 72−191.
(3) *Molecular Motors*; Schliwa, M., Ed.; Wiley-VCH: Weinheim, 2003.
(4) (a) Goodsell, D. S. *Bionanotechnology − Lessons from Nature*; Wiley: Hoboken, NJ, 2004. (b) Jones, R. A. L. *Soft Machines − Nanotechnology and life*; Oxford University Press: Oxford, 2005.

machines, in the form of chemical,[6] electrochemical,[7] or photochemical[8] inputs, is usually employed to bias the random thermal motion in order to obtain directed movements of the machine's components, although molecular systems wherein the energy input can be converted directly into controlled motion are available.[9] Another important requirement is the ability to detect and control the specific molecular actuations in response to the applied stimulation by monitoring suitable output signals.

Mechanically interlocked molecules, such as rotaxanes and catenanes,[10] are one of the most suitable candidates for molecular machines because (i) the mechanical bond allows a large variety of mutual arrangements of the molecular components, while conferring stability on the system; (ii) the interlocked architecture limits the amplitude of the intercomponent motion in the three dimensions; (iii) the stability of a specific arrangement (co-conformation[11]) is determined by the strength of the intercomponent interactions;[12] and (iv) such interactions can be modulated by external stimulation.[13] These systems, by virtue of their electrical properties and bi- or multistable behavior, are also attractive as nanoscale switches for molecular electronics[14] and nanoelectromechanical systems[15] (NEMS).

In a bistable [2]rotaxane, the competitive affinity of a macrocyclic ring with two distinct recognition sites on the thread component allows the macrocycle to translate between them, generating a nanoscale mechanical motion. Systems of this type, termed molecular shuttles,[16] constitute the most common implementation of the molecular machine concept with artificial molecules.[17] The primary requirement for generating such a controllable motion of the ring component and the detection of two separate translational isomers of a bistable [2]rotaxane is a large difference in the affinity of the macrocycle between the

(5) Astumian, R. D.; Hänggi, P. *Phys. Today* **2002**, *55* (11), 33−39.

(6) Recent examples of chemically-driven molecular machines: (a) Thordarson, P.; Bijsterveld, E. J. A.; Rowan, A. E.; Nolte, R. J. M. *Nature* **2003**, *424*, 915−918. (b) Badjić, J. D.; Balzani, V.; Credi, A.; Silvi, S.; Stoddart, J. F. *Science* **2004**, *303*, 1845−1849. (c) Hernandez, J. V.; Kay, E. R.; Leigh, D. A. *Science* **2004**, *306*, 1532−1537. (d) Garaudee, S.; Silvi, S.; Venturi, M.; Credi, A.; Flood, A. H.; Stoddart, J. F. *ChemPhysChem* **2005**, *6*, 2145−2152. (e) Liu, Y.; Flood, A. H.; Bonvallet, P. A.; Vignon, S. A.; Northrop, B. H.; Tseng, H.-R.; Jeppesen, J. O.; Huang, T. J.; Brough, B.; Baller, M.; Magonov, S.; Solares, S. D.; Goddard, W. A.; Ho, C.-M., Stoddart, J. F. *J. Am. Chem. Soc.* **2005**, *127*, 9745−9759. (f) Fletcher, S. P.; Dumur, F.; Pollard, M. M.; Feringa, B. L. *Science* **2005**, *310*, 80−82. (g) Leigh, D. A.; Lusby, P. J.; Slawin, A. M. Z.; Walker, D. B. *Chem. Commun.* **2005**, 4919−4921. (h) Nguyen, T. D.; Tseng, H.-R.; Celestre, P. C.; Flood, A. H.; Liu, Y.; Stoddart, J. F.; Zink, J. I. *Proc. Natl. Acad. Sci. U.S.A.* **2005**, *102*, 10029−10034. (i) Marlin, D. S.; Cabrera, D. G.; Leigh, D. A.; Slawin, A. M. Z. *Angew. Chem., Int. Ed.* **2006**, *45*, 77−83. (j) Marlin, D. S.; Cabrera, D. G.; Leigh, D. A.; Slawin, A. M. Z. *Angew. Chem., Int. Ed.* **2006**, *45*, 1385−1390. (k) Brough, B.; Northrop, B. H.; Schmidt, J. J.; Tseng, H.-R.; Houk, K. N.; Stoddart, J. F.; Ho, C.-M. *Proc. Natl. Acad. Sci. U.S.A.* **2006**, *103*, 8583−8588. (l) Cheng, K. W.; Lai, C. C.; Chiang, P. T.; Chiu, S. H. *Chem. Commun.* **2006**, 2854−2856. (m) Badjić, J. D.; Ronconi, C. M.; Stoddart, J. F.; Balzani, V.; Silvi, S.; Credi, A. *J. Am. Chem. Soc.* **2006**, *128*, 1489−1499. (n) Sindelar, V.; Silvi, S.; Kaifer, A. E. *Chem. Commun.* **2006**, 2185−2187. (o) Nguyen, T. D.; Leung, K. C. F.; Liong, M.; Pentecost, C. D.; Stoddart, J. F.; Zink, J. I. *Org. Lett.* **2006**, *8*, 3363−3366.

(7) Recent examples of electrochemically-driven molecular machines: (a) Altieri, A.; Gatti, F. G.; Kay, E. R.; Leigh, D. A.; Paolucci, F.; Slawin, A. M. Z.; Wong, J. K. Y. *J. Am. Chem. Soc.* **2003**, *125*, 8644−8654. (b) Steuerman, D. W.; Tseng, H.-R.; Peters, A. J.; Flood, A. H.; Jeppesen, J. O.; Nielsen, K. A.; Stoddart, J. F.; Heath, J. R. *Angew. Chem., Int. Ed.* **2004**, *43*, 6486−6491. (c) Poleschak, I.; Kern, J.-M.; Sauvage, J.-P. *Chem. Commun.* **2004**, 474−476. (d) Liu, Y.; Flood, A. H.; Stoddart, J. F. *J. Am. Chem. Soc.* **2004**, *126*, 9150−9151. (e) Katz, E.; Lioubashevsky, O.; Willner, I. *J. Am. Chem. Soc.* **2004**, *126*, 15520−15532. (f) Hawthorne, M. F.; Zink, J. I.; Skelton, J. M.; Bayer, M. J.; Liu, C.; Livshits, E.; Baer, R.; Neuhauser, D. *Science* **2004**, *303*, 1849−1851. (g) Tseng, H.-R.; Vignon, S. A.; Celestre, P. C.; Perkins, J.; Jeppesen, J. O.; Di Fabio, A.; Ballardini, R.; Gandolfi, M. T.; Venturi, M.; Balzani, V.; Stoddart, J. F. *Chem.−Eur. J.* **2004**, *10*, 155−172. (h) Iijima, T.; Vignon, S. A.; Tseng, H.-R.; Jarrosson, T.; Sanders, J. K. M.; Marchioni, F.; Venturi, M.; Apostoli, E.; Balzani, V.; Stoddart, J. F. *Chem.−Eur. J.* **2004**, *10*, 6375−6392. (i) Jeon, W. S.; Kim, E.; Ko, Y. H.; Hwang, I. H.; Lee, J. W.; Kim, S. Y.; Kim, H. J.; Kim, K. *Angew. Chem., Int. Ed.* **2005**, *44*, 87−91. (j) Letinois-Halbes, U.; Hanss, D.; Beierle, J. M.; Collin, J.-P.; Sauvage, J.-P. *Org. Lett.* **2005**, *7*, 5753−5756. (k) Sobransingh, D.; Kaifer, A. E. *Org. Lett.* **2006**, *8*, 3247−3250.

(8) Recent examples of photochemically driven molecular machines: (a) Brouwer, A. M.; Fazio, S. M.; Frochot, C.; Gatti, F. G.; Leigh, D. A.; Wong, J. K. Y.; Wurpel, G. W. H. *Pure Appl. Chem.* **2003**, *75*, 1055−1060. (b) van Delden, R. A.; Koumura, N.; Schoevaars, A.; Meetsma, A.; Feringa, B. L. *Org. Biomol. Chem.* **2003**, *1*, 33−35. (c) Perez, E. M.; Dryden, D. T. F.; Leigh, D. A.; Teobaldi, G.; Zerbetto, F. *J. Am. Chem. Soc.* **2004**, *126*, 12210−12211. (d) Abraham, W.; Grubert, L.; Grummt, U. W.; Buck, K. *Chem.−Eur. J.* **2004**, *10*, 3562−3568. (e) Mobian, P.; Kern, J.-M.; Sauvage, J.-P. *Angew. Chem., Int. Ed.* **2004**, *43*, 2392−2395. (f) van Delden, R. A.; ter Wiel, M. K. J.; Pollard, M. M.; Vicario, J.; Koumura, N.; Feringa, B. L. *Nature* **2005**, *437*, 1337−1340. (g) Wang, Q.-C.; Qu, D.-H.; Ren, J.; Chen, K.; Tian, H. *Angew. Chem., Int. Ed.* **2004**, *43*, 2661−2665. (h) Collin, J.-P.; Jouvenot, D.; Koizumi, M.; Sauvage, J.-P. *Eur. J. Inorg. Chem.* **2005**, 1850−1855. (i) Qu, D.-H.; Wang, Q.-C.; Tian, H. *Angew. Chem., Int. Ed.* **2005**, *44*, 5296−5299. (j) Murakami, H.; Kawabuchi, A.; Matsumoto, R.; Ido, T.; Nakashima, N. *J. Am. Chem. Soc.* **2005**, *127*, 15891−15899. (k) Murakami, H.; Kawabuchi, A.; Matsumoto, R.; Ido, T.; Nakashima, N. *J. Am. Chem. Soc.* **2005**, *127*, 15891−15899. (l) Muraoka, T.; Kinbara, K.; Aida, T. *Nature* **2006**, *440*, 512−515. (m) Vicario, J.; Walko, M.; Meetsma, A.; Feringa, B. L. *J. Am. Chem. Soc.* **2006**, *128*, 5127−5135. (n) Balzani, V.; Clemente-León, M.; Credi, A.; Ferrer, B.; Venturi, M.; Flood, A. H.; Stoddart, J. F. *Proc. Natl. Acad. Sci. U.S.A.* **2006**, *103*, 1178−1183. (o) Balzani, V.; Clemente-León, M.; Credi, A.; Semeraro, M.; Venturi, M.; Tseng, H.-R.; Wenger, S.; Saha, S.; Stoddart, J. F. *Aust. J. Chem.* **2006**, *59*, 193−206.

(9) Katz, E.; Baron, R.; Willner, I.; Richke, N.; Levine, R. D. *Chem. Phys. Chem.* **2005**, *6*, 2179−2189.

(10) *Catenanes, Rotaxanes and Knots*; Sauvage, J.-P., Dietrich-Buchecker, C., Eds.; Wiley-VCH: Weinheim, 1999.

(11) For a definition of co-conformation, see: Fyfe, M. C. T.; Stoddart, J. F. *Acc. Chem. Res.* **1997**, *30*, 393−401.

(12) (a) Busch, D. H.; Stephenson, N. A. *Coord. Chem. Rev.* **1990**, *100*, 119−154. (b) Lindsey, J. S. *New J. Chem.* **1991**, *15*, 153−180. (c) Philp, D.; Stoddart, J. F. *Synlett* **1991**, 445−458. (d) Hunter, C. A. *J. Am. Chem. Soc.* **1992**, *114*, 5303−5311. (e) Anderson, S.; Anderson, H. L.; Sanders, J. K. M. *Acc. Chem. Res.* **1993**, *26*, 469−475. (f) Bisson, A. P.; Carver, F. J.; Hunter, C. A.; Waltho, J. P. *J. Am. Chem. Soc.* **1994**, *116*, 10292−10293. (g) Hunter, C. A. *Angew. Chem., Int. Ed. Engl.* **1995**, *34*, 1079−1081. (h) Schneider, J. P.; Kelly, J. W. *Chem. Rev.* **1995**, *95*, 2169−2187. (i) Philp, D.; Stoddart, J. F. *Angew. Chem., Int. Ed. Engl.* **1996**, *35*, 1154−1196. (j) Kolchinski, A. G.; Alcock, N. W.; Roesner, R. A.; Busch, D. H. *Chem. Commun.* **1998**, 1437−1438. (k) Fujita, M. *Acc. Chem. Res.* **1999**, *32*, 53−61. (l) Rebek, J., Jr. *Acc. Chem. Res.* **1999**, *32*, 278−286. (m) *Templated Organic Synthesis*; Diederich, F., Stang, P. J., Eds.; Wiley-VCH: Weinheim, 1999. (n) Nakash, M.; Watson, Z. C.; Feeder, N.; Teat, S. J.; Sanders, J. K. M. *Chem.−Eur. J.* **2000**, *6*, 2112−2119. (o) Sanders, J. K. M. *Pure Appl. Chem.* **2000**, *72*, 2265−2274. (p) Bong, D. T.; Clark, T. D.; Granja, J. R.; Ghadiri, M. R. *Angew. Chem.* **2001**, *113*, 1016−1041; *Angew. Chem., Int. Ed.* **2001**, *40*, 988−1011. (q) Prins, L. J.; Reinhoudt, D. N.; Timmerman, P. *Angew. Chem., Int. Ed.* **2001**, *40*, 2382−2426. (r) Seidel, S. R.; Stang, P. J. *Acc. Chem. Res.* **2002**, *35*, 972−983. (s) Stoddart, J. F.; Tseng, H.-R. *Proc. Natl. Acad. Sci. U.S.A.* **2002**, *99*, 4797−4800. (t) Furlan, R. L. E.; Otto, S.; Sanders, J. K. M. *Proc. Natl. Acad. Sci. U.S.A.* **2002**, *99*, 4801−4804. (u) Joester, D.; Walter, E.; Losson, M.; Pugin, R.; Merkle, H. P.; Diederich, F. *Angew. Chem.* **2003**, *115*, 1524−1528; *Angew. Chem., Int. Ed.* **2003**, *42*, 1486−1490. (v) Hogg, L.; Leigh, D. A.; Lusby, P. J.; Morelli, A.; Parsons, S.; Wong, J. K. Y. *Angew. Chem., Int. Ed.* **2004**, *43*, 1218−1221. (w) Zheng, X.; Mulcahy, M. E.; Horinek, D.; Galeotti, F.; Magnera, T. F.; Michl, J. *J. Am. Chem. Soc.* **2004**, *126*, 4540−4542.

(13) Balzani, V.; Credi, A.; Silvi, S.; Venturi, M. *Chem. Soc. Rev.* **2006**, *35*, 1135−1149.

(14) Bistable catenanes and rotaxanes have been employed as switches in a range of devices and across different environments. See: (a) Collier, C. P.; Mattersteig, G.; Wong, E. W.; Luo, Y.; Beverly, K.; Sampaio, J.; Raymo, F. M.; Stoddart, J. F.; Heath, J. R. *Science*, **2000**, *289*, 1172−1175. (b) Pease, A. R.; Jeppesen, J. O.; Stoddart, J. F.; Luo, Y.; Collier, C. P.; Heath, J. R. *Acc. Chem. Res.* **2001**, *34*, 434−444. (c) Luo, Y.; Collier, C. P.; Jeppesen, J. O.; Neilsen, K. A.; DeIonno, E.; Ho, G.; Perkins, J.; Tseng, H.-R.; Yamamoto, T.; Stoddart, J. F.; Heath, J. R. *Chem. Phys. Chem.* **2002**, *3*, 519−525. (d) Diehl, M. R.; Steuerman, D. W.; Tseng, H.-R.; Vignon, S. A.; Star, A.; Celestre, P. C.; Stoddart, J. F.; Heath, J. R. *Chem. Phys. Chem.* **2003**, *4*, 1335−1339. (e) Tseng, H.-R.; Wu, D.; Fang, N.; Zhang, X.; Stoddart, J. F. *Chem. Phys. Chem.* **2004**, *5*, 111−116. (f) Steuerman, D. W.; Tseng, H.-R.; Peters, A. J.; Flood, A. H.; Jeppesen, J. O.; Nielsen, K. A.; Stoddart, J. F.; Heath, J. R. *Angew. Chem., Int. Ed.* **2004**, *43*, 6486−6491. (g) Flood, A. H.; Peters, A. J.; Vignon, S. A.; Steuerman, D. W.; Tseng, H.-R.; Kang, S.; Heath, J. R.; Stoddart, J. F. *Chem.−Eur. J.* **2004**, *10*, 6558−6464. (h) Flood, A. H.; Stoddart, J. F.; Steuerman, D. W.; Heath, J. R. *Science* **2004**, *306*, 2055−2056. (i) Jang, S. S.; Kim, Y. H.; Goddard, W. A., III; Flood, A. H.; Laursen, B. W.; Tseng, H.-R.; Stoddart, J. F.; Jeppesen, J. O.; Choi, J. W.; Steuerman, D. W.; DeIonno, E.; Heath, J. R. *J. Am. Chem. Soc.* **2005**, *127*, 1563−1575. (j) Green, J. E.; Choi, J. W.; Boukai, A.; Bunimovich, Y.; Johnston-Halperin, E.; DeIonno, E.; Luo, Y.; Sheriff, B. A.; Xu, K.; Shin, Y. S.; Tseng, H.-R.; Stoddart, J. F.; Heath, J. R. *Nature* **2007**, *445*, 414−417.

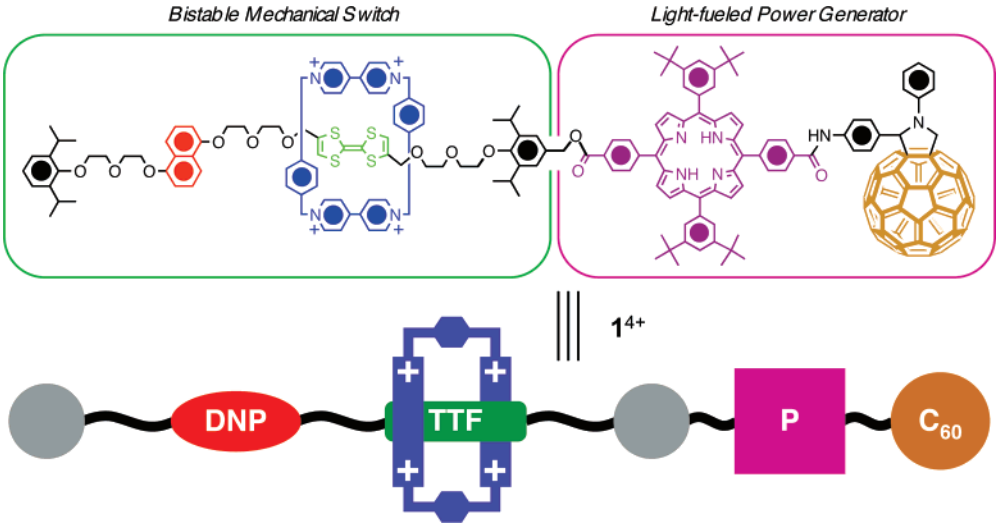

Figure 1. Structural formula and graphical representation of the multicomponent rotaxane $\mathbf{1}^{4+}$.

competing stations on the thread. A free energy difference greater than 1.3 kcal mol^{-1} between two translational isomers ensures[7e] that, at room temperature, in more than 90% of rotaxane molecules the ring component resides around one recognition site over the other. In order to generate significant translational motion of the ring within the interlocked molecules, a variety of external signals, such as chemical, electrochemical, and/or photoelectrochemical stimuli[6−8] have been successfully employed.

For a variety of reasons, light is one of the most important means of supplying energy to nanodevices, including molecular machines.[8,18] Important directions for the design of light-powered molecular machines are provided by research in artificial photosynthesis.[19] For instance, donor−chromophore−acceptor molecular triads comprising a π-electron donor (e.g., tetrathiafulvalene (TTF), π-extended TTF, ferrocene, dihydropyrene, carotene), a chromophoric porphyrin unit, and a π-electron acceptor (e.g., C_{60}, quinones) have been shown to (i) generate photocurrent,[20] (ii) perform active transportation of H^+ and Ca^{2+} ions across artificial lipid membranes,[21,22] and (iii) synthesize ATP,[21b,c] all by harnessing light energy to generate an electron flow which builds up an electrochemical gradient at the nanoscale. In our early studies, we have utilized[23] a TTF−P−C_{60}-based photoactive triad to verify that light energy generates the charge-separated state with a singly oxidized TTF component and singly reduced C_{60} component, $TTF^+-P-C_{60}^-$. The ensuing photocurrent was used as a power supply to drive a supramolecular machine in the form of a pseudorotaxane. Integration of such a light-harvesting moiety into an interlocked molecular system, such as a two-station TTF−DNP-based

(15) (a) Long, B.; Nikitin, K.; Fitzmaurice, D. *J. Am. Chem. Soc.* **2003**, *125*, 15490−15498. (b) Hernandez, R.; Tseng, H.-R.; Wong, J. W.; Stoddart, J. F.; Zink, J. I. *J. Am. Chem. Soc.* **2004**, *126*, 3370−3371. (c) Huang, T. J.; Tseng, H.-R.; Sha, L.; Lu, W.; Brough, B.; Flood, A. H.; Yu, B.-D.; Celestre, P. C.; Chang, J. P.; Stoddart, J. F.; Ho, C.-M. *Nano Lett.* **2004**, *4*, 2065−2071. (d) Lee, I. C.; Frank, C. W.; Yamamoto, T.; Tseng, H.-R.; Flood, A. H.; Stoddart, J. F.; Jeppesen, J. O. *Langmuir* **2004**, *20*, 5809−5818. (e) Huang, T. J.; Brough, B.; Ho, C.-M.; Liu, Y.; Flood, A. H.; Bonvallet, P. A.; Tseng, H.-R.; Stoddart, J. F.; Baller, M.; Magonov, S. *Appl. Phys. Lett.* **2004**, *85*, 5391−5393. (f) Katz, E.; Sheeney-Haj-Ichia, L.; Willner, I. *Angew. Chem., Int. Ed.* **2004**, *43*, 3292−3300. (g) Lioubashevski, O.; Chegel, V. I.; Patolsky, F.; Katz, E.; Willner, I. *J. Am. Chem. Soc.* **2004**, *126*, 7133−7143. (h) Huang, T. J.; Flood, A. H.; Brough, B.; Liu, Y.; Bonvallet, P. A.; Kang, S. S.; Chu, C. W.; Guo, T. F.; Lu, W. X.; Yang, Y; Stoddart, J. F.; Ho, C.-M. *IEEE T. Autom. Sci. Eng.* **2006**, *3*, 254−259. (i) Nguyen, T. D.; Liu, Y.; Saha, S.; Leung, K. C.-F.; Stoddart, J. F.; Zink, J. I. *J. Am. Chem. Soc.* **2007**, *129*, 626−634.
(16) (a) Anelli, P.-L.; Spencer, N.; Stoddart, J. F. *J. Am. Chem. Soc.* **1991**, *113*, 5131−5133. (b) Bissell, R. A.; Córdova, E.; Kaifer, A. E.; Stoddart, J. F. *Nature* **1994**, *369*, 133−137.
(17) Molecular shuttles: (a) Anelli, P.-L., et al. *Chem.−Eur. J.* **1997**, *3*, 1136−1150. (b) Ashton, P. R.; Ballardini, R.; Balzani, V.; Baxter, I.; Credi, A.; Fyfe, M. C. T.; Gandolfi, M. T.; Gómez-López, M.; Martínez-Díaz, M.-V.; Piersanti, A.; Spencer, N.; Stoddart, J. F.; Venturi, M.; White, A. J. P.; Williams, D. J. *J. Am. Chem. Soc.* **1998**, *120*, 11932−11942. (c) Leigh, D. A.; Troisi, A.; Zerbetto, F. *Angew. Chem., Int. Ed.* **2000**, *39*, 350−353. (d) Jeppesen, J. O.; Nielsen, K. A.; Perkins, J.; Vignon, S. A.; Di Fabio, A.; Ballardini, R.; Gandolfi, M. T.; Venturi, M.; Balzani, V.; Becher, J.; Stoddart, J. F. *Chem.−Eur. J.* **2003**, *9*, 2982−3007. (e) Jeppesen, J. O.; Vignon, S. A.; Stoddart, J. F. *Chem.−Eur. J.* **2003**, *9*, 4611−4625. (f) Laursen, B. W.; Nygaard, S.; Jeppesen, J. O.; Stoddart, J. F. *Org. Lett.* **2004**, *6*, 4167−4170. (g) Jeppesen, J. O.; Nygaard, S.; Vignon, S. A.; Stoddart, J. F. *Eur. J. Org. Chem.* **2005**, 196−220. For more examples of artificial molecular machines, see refs 6d,e,h−l, 7a,g,h, 8a,c,i,l,m, and 9.
(18) (a) Balzani, V. *Photochem. Photobiol. Sci.* **2003**, *2*, 459−476. (b) Credi, A. *Aust. J. Chem.* **2006**, *59*, 157−169. (c) Saha, S.; Stoddart, J. F. *Chem. Soc. Rev.* **2007**, *36*, 77−92.
(19) (a) Wasielewski, M. R. *Chem. Rev.* **1992**, *92*, 435−461. (b) Gust, D.; Moore, T. A.; Moore, A. L. *Acc. Chem. Res.* **1993**, *26*, 198−205. (c) Gust, D.; Moore, T. A.; Moore, A. L. *Acc. Chem. Res.* **2001**, *34*, 40−48. (d) Guldi, D. M. *Chem. Soc. Rev.* **2002**, *31*, 22−36. (e) Hammarström, L. *Curr. Opin. Chem. Biol.* **2003**, *7*, 666−673. (f) Alstrum-Acevedo, J. H.; Brennaman, M. K.; Meyer, T. J. *Inorg. Chem.* **2005**, *44*, 6802−6827. (g) Wiberg, J.; Guo, L. J.; Pettersson, K.; Nilsson, D.; Ljungdahl, T.; Martensson, J.; Albinsson, B. *J. Am. Chem. Soc.* **2007**, *129*, 155−163.
(20) (a) Fujitsuka, M.; Ito, O.; Imahori, H.; Yamada, K.; Yamada, H.; Sakata, Y. *Chem. Lett.* **1999**, 721−722. (b) Imahori, H.; Yamada, H.; Ozawa, S.; Sakata, Y.; Ushida, K. *Chem. Commun.* **1999**, *13*, 1165−1166. (c) Imahori, H.; Yamada, H.; Nishimura, Y.; Yamazaki, I.; Sakata, Y. *J. Phys. Chem. B* **2000**, *104*, 2099−2108. (d) Guldi, D. M. *Chem. Commun.* **2000**, 321−327. (e) Herranz, M. Á.; Illescas, B.; Martín, N.; Luo, C.; Guldi, D. M. *J. Org. Chem.* **2000**, *65*, 5728−5738. (f) Martín, N.; Sánchez, L.; Herranz, M. Á.; Guldi, D. M. *J. Phys. Chem. A* **2000**, *104*, 4648−4657. (g) Li, H.; Jeppesen, J. O.; Levillain, E.; Becher, J. *Chem. Commun.* **2003**, *7*, 846−847. (h) Sánchez, L.; Perez, I.; Martín, N.; Guldi, D. M. *Chem.−Eur. J.* **2003**, *9*, 2457−2468. (i) Guldi, D. M.; Luo, C.; Swartz, A.; Gomez, R.; Segura, J. L.; Martín, N. *J. Phys. Chem. A* **2004**, *4*, 455−467. (j) Imahori, H.; Mori, Y.; Matano, Y. *J. Photochem. Photobiol., C* **2004**, *4*, 51−83. (k) Imahori, H.; Kimura, M.; Hosomizu, K.; Fukuzumi, S. *J. Photochem. Photobiol., A* **2004**, *166*, 57−62. (l) Guldi, D. M.; Imahori, H.; Tamaki, K.; Kashiwagi, Y.; Yamada, H.; Sakata, Y.; Fukuzumi, S. *J. Phys. Chem. A* **2004**, *108*, 541−548. (m) Nishikawa, H.; Kojima, S.; Kodama, T.; Ikemoto, I.; Suzuki, S.; Kikuchi, K.; Fujitsuka, M.; Luo, H.; Araki, Y.; Ito, O. *J. Phys. Chem. A* **2004**, *108*, 1881−1890. (n) de la Torre, G.; Giacalone, F.; Segura, J. L.; Martín, N.; Guldi, D. M. *Chem.−Eur. J.* **2005**, *11*, 1267−1280.
(21) (a) Steinberg-Yfrach, G.; Liddell, P. A.; Hung, S.-C.; Moore, A. L.; Gust, D.; Moore, T. A. *Nature* **1997**, *385*, 239−241. (b) Steinberg-Yfrach, G.; Rigaud, J.-L.; Durantini, E. N.; Moore, A. L.; Gust, D.; Moore, T. A. *Nature* **1998**, *392*, 479−482. (c) Gust, D.; Moore, T. A.; Moore, A. L. *Acc. Chem. Res.* **2001**, *34*, 40−48.
(22) Bennett, I. M.; Farfano, H. M. V.; Bogani, F.; Primak, A.; Liddell, P. A.; Otero, L.; Sereno, L.; Silber, J. J.; Moore, A. L.; Moore, T. A.; Gust, D. *Nature* **2002**, *420*, 398−401.
(23) (a) Saha, S.; Johansson, L. E.; Flood, A. H.; Tseng, H.-R.; Zink, J. I.; Stoddart, J. F. *Small* **2005**, *1*, 87−90. (b) Saha, S.; Johansson, E.; Flood, A. H.; Tseng, H. R.; Zink, J. I.; Stoddart, J. F. *Chem.−Eur. J.* **2005**, *11*, 6846−6858.

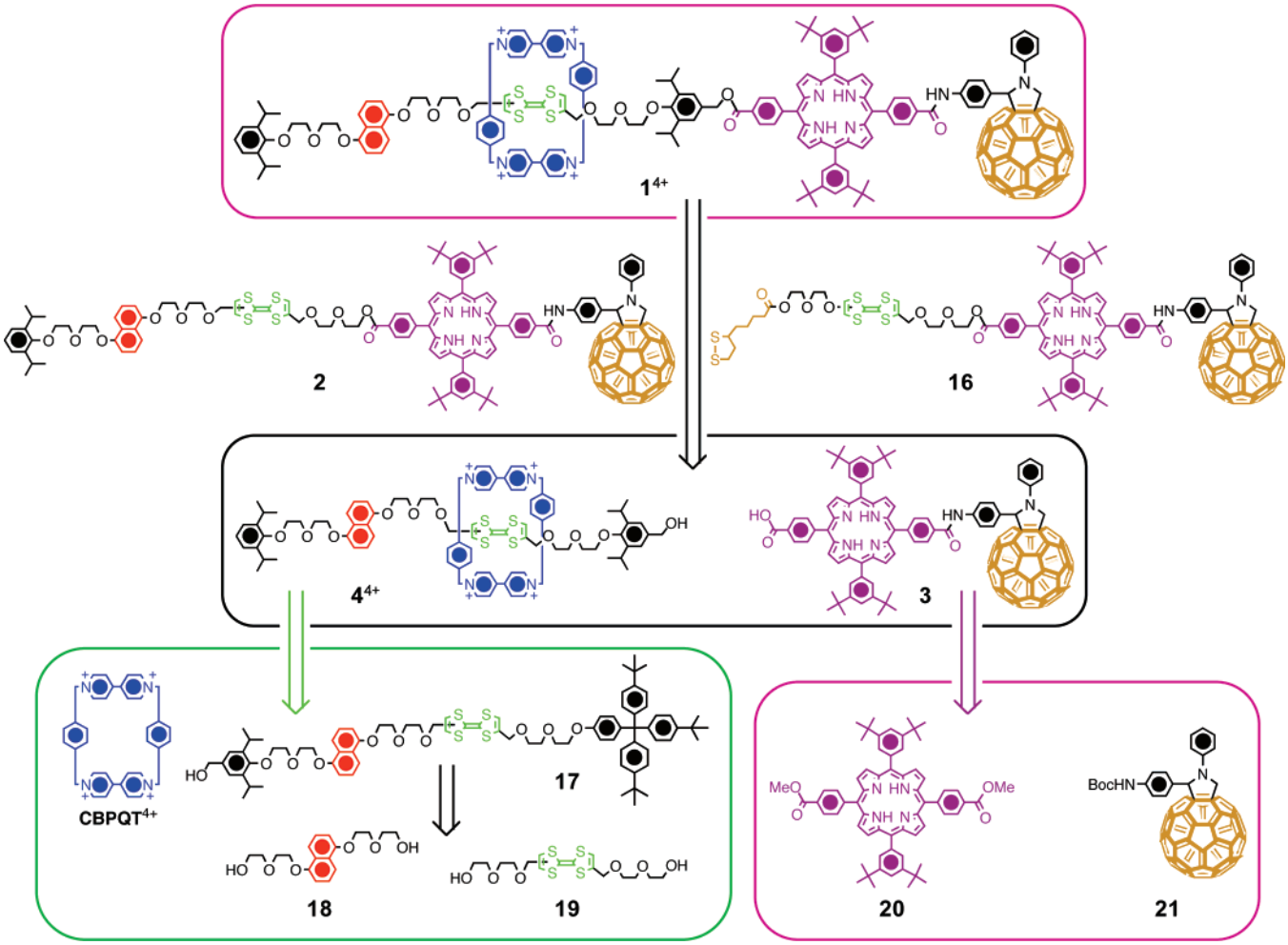

Figure 2. Progeny of the multicomponent rotaxane. Structural formulas of the multicomponent [2]rotaxane $\mathbf{1}^{4+}$, the tetrad **2**, the dyad **3**, the bistable [2]rotaxane $\mathbf{4}^{4+}$, and the triad **16** as well as their retrosynthetic scheme involving dumbbell-shaped compound **17**, the DNP derivative **18**, the TTF derivative **19**, the free-base tetraarylporphyrin **20**, and the fulleropyrrolidine **21**.

bistable [2]rotaxane,[14,17d−g] may lead to the photochemical control of the shuttling motion on account of photoinduced electron transfer (PET) processes within the multicomponent rotaxane.

In this paper we report the design, modular synthesis, and properties of the photoactive bistable [2]rotaxane $\mathbf{1}^{4+}$ (Figure 1), its dumbbell-shaped thread component **2**, and model compounds (Figure 2) for the functional units incorporated into its structure, with the primary objective of establishing whether the mechanical switching properties of the TTF−DNP-based rotaxane motif are retained in this multicomponent system. UV−vis−NIR Absorption spectroscopy, electrochemical methods, and the coupling of the two (spectroelectrochemistry) have been employed to characterize the intercomponent interactions in the rotaxane and to investigate the redox-induced shuttling. The light-driven operation of $\mathbf{1}^{4+}$ as a molecular shuttle requires extensive photophysical studies and will be investigated in the course of time.

Design

Molecular machines are structurally organized, functionally integrated multicomponent systems designed to perform controllable mechanical-like motions of their components when fed by an appropriate energy source.[1,2] The energy supply for molecular machines is a problem of primary importance. The most common way to power molecular machines is through the addition of a fuel capable of causing an appropriate chemical reaction that eventually causes the motion, as it happens in the ATP-powered biological molecular motors. Such an approach, which is strongly related to operation in solution, requires the continuous supply of fuel molecules and implies the formation of waste products. Nature also shows, however, that the energy needed to sustain the machinery of life is ultimately provided by sunlight via a charge-separation process, i.e., the generation of an electrochemical potential.[24] Photon inputs can indeed cause the occurrence of endergonic chemical reactions in suitably designed artificial molecular systems that can make a machine work without the generation of waste products. As pointed out elsewhere,[1,2,13,18] light inputs have other advantages over a chemical or electrochemical energy supply.

Taking advantage of our past experience on photochemically driven molecular machines,[25] culminated by the construction[26] of an autonomous molecular shuttle powered by sunlight,[8l,m] we came up with the design (Figure 1) of the multicomponent rotaxane $\mathbf{1}^{4+}$. This system entails the integration of (1) a light-fueled power generator, capable of converting the photon energy

(24) (a) *Oxygenic Photosynthesis: the Light Reactions*; Ort, D. R., Yocum, C. F., Eds.; Kluwer: Dordrecht, 1996. (b) Rhee, K.-H.; Morriss, E. P.; Barber, J.; Kühlbrandt, W. *Nature* **1998**, *396*, 283−286. (c) Renger, T.; Marcus, R. A. *J. Phys. Chem. B* **2002**, *106*, 1809−1819.

into an electrochemical potential, and (2) a mechanical switch, capable of utilizing such a photochemically generated driving force to bring about controllable molecular shuttling motions. The light-fueled power generator is a dyad comprising (i) a fullerene (C_{60}) component and (ii) a tetraarylporphyrin (P) unit. C_{60} was selected because of its electron-accepting character and for the low electronic reorganization energy[27] on account of its three-dimensional spherical geometry. Taken together, these two features make the C_{60} unit a remarkably efficient acceptor in electron-transfer systems and a most attractive component in artificial photosynthetic devices.[19−23] Porphyrins are the principal chromophores chosen by Nature for harvesting sunlight.[28] Free-base porphyrins are widely used in charge-separation molecular devices[19,23a−e,29] because they can act as electron donors in the excited state. Furthermore, their absorption spectrum,[30] while distributed across most of the visible spectral region, shows a sharp and very intense peak (Soret band, ca. 420 nm) which is isolated conveniently from the absorption bands of the other components present in $\mathbf{1}^{4+}$, thereby allowing selective excitation of the porphyrin unit in the assembly. The light harvesting dyad moiety **3** (Figure 2) of the multicomponent rotaxane was prepared[23] by attaching the C_{60} unit covalently with the porphyrin unit.

The mechanical switch is a redox-active bistable [2]rotaxane moiety that consists of a molecular thread containing (i) tetrathiafulvalene (TTF) and (ii) dioxynaphthalene (DNP) units as π-electron-donating stations, separated by a poly(ethylene glycol) spacer, and of (iii) a tetracationic cyclobis(paraquat-*p*-phenylene) ($CBPQT^{4+}$) π-electron-accepting tetracationinc cyclophane (hereafter called the ring). To prevent the $CBPQT^{4+}$ ring from slipping off and from approaching the porphyrin unit, bulky 2,6-diisopropyl aryl stoppers were placed at both ends of the thread. The model compound for such a mechanical switch is the bistable rotaxane $\mathbf{4}^{4+}$ (Figure 2). The competitive noncovalent-binding of the $CBPQT^{4+}$ ring with two recognition sites, namely TTF and DNP, on the thread component can be exploited to induce its shuttling between these sites.[14,17d−g] In the starting, rest state of the multicomponent rotaxane, a strong $\pi-\pi$ charge-transfer (CT) interaction between the $CBPQT^{4+}$ ring and the electron-rich TTF unit, reinforced by C−H···O interactions,[31] provides a thermodynamic advantage for the ring to reside[32] on the TTF station. The stabilizing interactions between the TTF station and the ring can be turned off by oxidation of the TTF component, at which stage the second π-electron-donating DNP station provides a higher affinity to the $CBPQT^{4+}$ ring. Thus, a combination of the electrostatic repulsion of the $CBPQT^{4+}$ ring away from the oxidized TTF and the stabilizing interactions afforded by the DNP station induces a molecular movement of the ring from its initial TTF station to the DNP station, according to a sort of "push−pull" mechanism possibly assisted by the ambient thermal energy. Regeneration of the neutral TTF unit by a reduction process gives rise to a metastable co-conformation which may relax back thermally to the rest state through the return of the ring to the original TTF station. The switching processes of the $CBPQT^{4+}$ ring in TTF−DNP-based bistable interlocked molecules in response to chemical and electrochemical inputs are now well-understood phenomena.[14,17d−g,32,33]

Since it is known[34] that visible light excitation of the porphyrin unit in TTF−P−C_{60} triads leads to a TTF^{+}−P−C_{60}^{-} charge-separated state, we envisaged that the oxidation of the TTF unit in the rotaxane $\mathbf{1}^{4+}$ could be obtained as a result of a sequence of electron-transfer processes initiated by light. The reduction of TTF^{+} back to neutral TTF will then be accomplished by back electron transfer from the C_{60}^{-} unit. Therefore, visible light excitation of $\mathbf{1}^{4+}$ is expected to trigger a "power stroke" leading to ring displacement from the TTF to the DNP station. Subsequent charge recombination, by restoring the starting electronic distribution, triggers the "recovery stroke" which leads to shuttling of the ring back to the TTF station and overall reset of the machine. Thus, the light-driven operation of $\mathbf{1}^{4+}$ as a molecular shuttle with autonomous behavior relies on a complex sequence of electronic and nuclear motions that must be carefully synchronized, similarly to what happens for the four strokes of an internal combustion engine. In this paper, we will not discuss in detail the requirements and features of the light-driven mechanism. Rather, we will focus our discussion on a key process for the operation of multicomponent rotaxane $\mathbf{1}^{4+}$, namely, the oxidation of the TTF unit by chemical and electrochemical means.

Results and Discussions

Syntheses. The multicomponent rotaxane $\mathbf{1}^{4+}$ and the corresponding dumbbell compound **2** were synthesized in a modular fashion, starting with the syntheses of the active components, and by putting them together to obtain these target molecules as illustrated in Schemes 1−3. The P−C_{60} dyad **3**[23] and compounds **5**,[35] **7**,[36] **10**,[7g] **13**,[37] and $\mathbf{15}^{2+}$[38] were prepared

(25) (a) Ballardini, R.; Balzani, V.; Gandolfi, M. T.; Prodi, L.; Venturi, M.; Philp, D.; Ricketts, H. G.; Stoddart, J. F. *Angew. Chem., Int. Ed.* **1993**, *32*, 1301−1303. (b) Ashton, P. R., et al. *Chem.−Eur. J.* **1997**, *3*, 152−170. (c) Ashton, P. R.; Ballardini, R.; Balzani, V.; Constable, E. C.; Credi, A.; Kocian, O.; Langford, S. J.; Preece, J. A.; Prodi, L.; Schofield, E. R.; Spencer, N.; Stoddart, J. F.; Wenger, S. *Chem.−Eur. J.* **1998**, *4*, 2413−2422. (d) Ashton, P. R.; Balzani, V.; Kocian, O.; Prodi, L.; Spencer, N.; Stoddart, J. F. *J. Am. Chem. Soc.* **1998**, *120*, 11190−11191.

(26) Ashton, P. R.; Ballardini, R.; Balzani, V.; Credi, A.; Dress, R.; Ishow, E.; Kocian, O.; Preece, J. A.; Spencer, N.; Stoddart, J. F.; Venturi, M.; Wenger, S. *Chem.−Eur. J.* **2000**, *6*, 3558−3574.

(27) Imahori, H.; Hagiwara, K.; Aoki, M.; Akiyama, T.; Taniguchi, S.; Okada, T.; Shirakawa, M.; Sakata, Y. *J. Am. Chem. Soc.* **1996**, *118*, 11771−11782.

(28) (a) McDermott, G.; Prince, S. M.; Freer, A. A.; Hawthornthwaite-Lawless, A. M.; Papiz, M. Z.; Cogdell, R. J.; Isaacs, N. W. *Nature* **1995**, *374*, 517−521. (b) Pullerits, T.; Sundström, V. *Acc. Chem. Res.* **1996**, *29*, 381−389. (c) Balaban, T. S. *Acc. Chem. Res.* **2005**, *38*, 612−623.

(29) Recent examples: (a) Nakamura, T.; Ikemoto, J.; Fujitsuka, M.; Araki, Y.; Ito, O.; Takimiya, K.; Aso, Y.; Otsubo, T. *J. Phys. Chem. B* **2005**, *109*, 14365−14374. (b) Kobori, Y.; Yamauchi, S.; Akiyama, K.; Tero-Kubota, S.; Imahori, H.; Fukuzumi, S.; Norris, J. R. *Proc. Natl. Acad. Sci. U.S.A.* **2005**, *102*, 10017−10022. (c) D'Souza, F.; Chitta, R.; Gadde, S.; Zandler, M. E.; McCarty, A. L.; Sandanayaka, A. S. D.; Araki, Y.; Ito, O. *J. Phys. Chem. A* **2006**, *110*, 4338−4347.

(30) Kalyanasundaram, K. *Photochemistry of Polypyridine and Porphyrin Complexes*; Academic Press: London, 1991.

(31) (a) Asakawa, M.; Ashton, P. R.; Balzani, V.; Credi, A.; Mattersteig, G.; Matthews, O. A.; Monatalti, M.; Spencer, N.; Stoddart, J. F.; Venturi, M.; *Chem.−Eur. J.* **1997**, *3*, 1992−1996. (b) Balzani, V.; Credi, A.; Mattersteig, G.; Matthews, O. A.; Raymo, F. M.; Stoddart, J. F.; Venturi, M.; White, A. J. P.; Williams, D. J. *J. Org. Chem.* **2000**, *65*, 1924−1936. (c) Liu, Y.; Flood, A. H.; Moskowitz, R. R.; Stoddart, J. F. *Chem.−Eur. J.* **2005**, *11*, 369−385.

(32) Tseng, H.-R.; Vignon, S. A.; Stoddart, J. F. *Angew. Chem., Int. Ed.* **2003**, *42*, 1491−1495.

(33) Ceccarelli, M.; Mercuri, F.; Passerone, D.; Parrinello, M. *J. Phys. Chem.* **2005**, *109*, 17094−17099.

(34) (a) Liddell, P. A.; Kodis, G.; de la Garza, L.; Bahr, J. L.; Moore, A. L.; Moore, T. A.; Gust, D. *Helv. Chim. Acta* **2001**, *84*, 2765−2783. (b) Kodis, G.; Liddell, P. A.; de la Garza, L.; Moore, A. L.; Moore, T. A.; Gust, D. *J. Mater. Chem.* **2002**, *12*, 2100−2108.

(35) (a) Khalil, B.; Calinaud, P.; Gelas, J.; Ghobsi, M. *Carb. Res.* **1994**, *264*, 33−44. (b) Xie, H.; Wu, S. *Supramol. Chem.* **2001**, *13*, 546−556.

(36) Becher, J.; Matthews, O.; Nielsen, K.; Mogens, B.; Raymo, F. M.; Stoddart, J. F. *Synlett* **1999**, 330−332.

(37) Roth, B.; Baccanari, D. P.; Sigel, C. W.; Hubbell, J. P.; Eaddy, J.; Kao, J. C.; Grace, M. E.; Rauckman, B. S. *J. Med. Chem.* **1988**, *31*, 122−129.

Scheme 1. Preparation of the [2]Rotaxane **4**·4PF$_6$

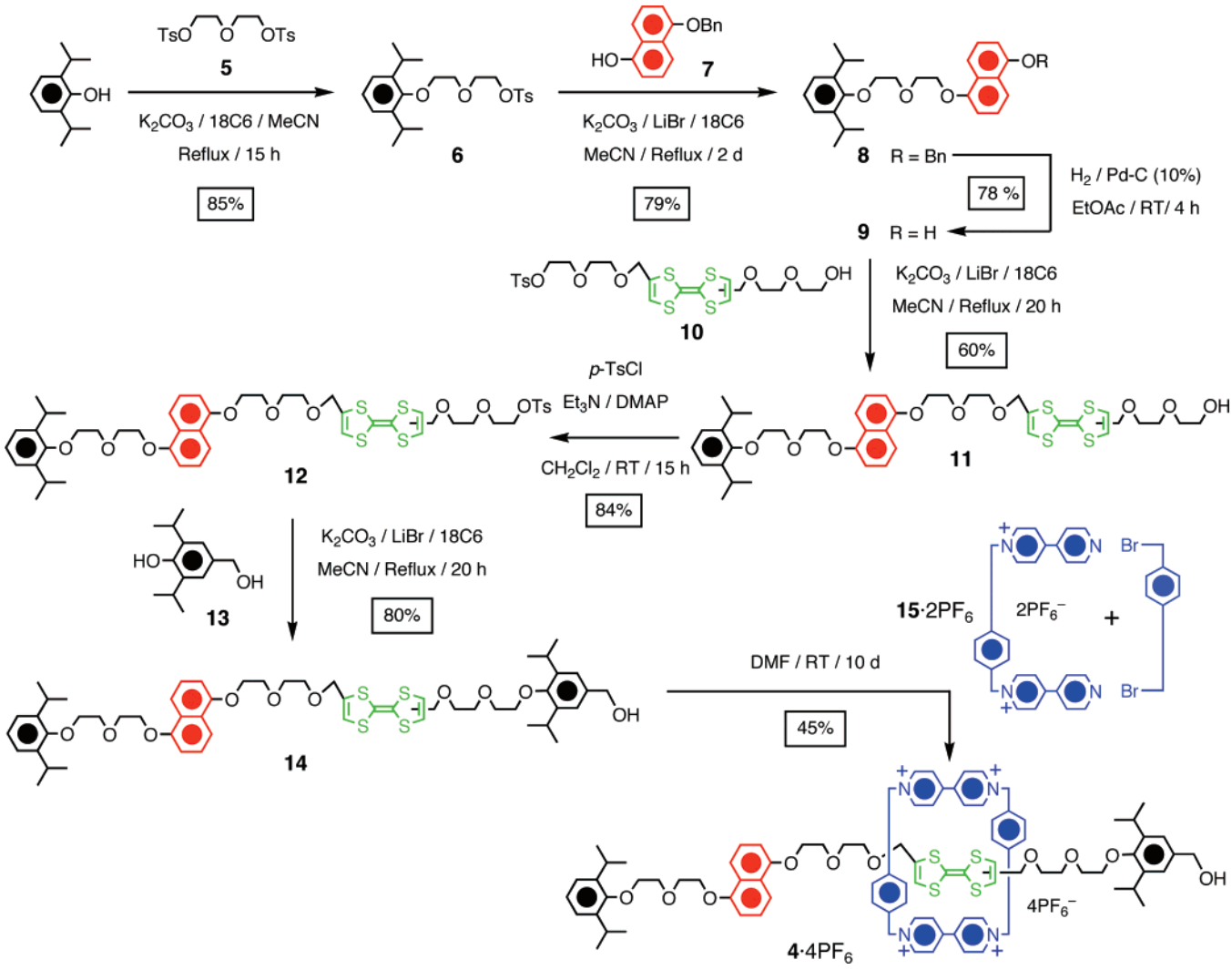

according to literature procedures. The bistable [2]rotaxane **4**$^{4+}$ was synthesized (Scheme 1) by a template-directed macrocyclization to form the CBPQT^{4+} ring around the templating TTF component. Finally, the P−C$_{60}$ dyad **3** with a terminal benzylic alcohol functionality and the rotaxane **4**$^{4+}$ bearing a carboxylic acid group were stitched together (Scheme 2) by an esterification to furnish the multicomponent [2]rotaxane **1**$^{4+}$.

Synthesis of Rotaxane 4·4PF$_6$: The synthesis of the rotaxane **4**$^{4+}$ is outlined in Scheme 1. The bis-tosylate **5**[35] was etherified with 1 equiv of 2,6-diisopropyl phenol in the presence of K_2CO_3 to obtain the monotosylate **6** in 85% yield. Etherification of the monobenzyl protected 1,5-dioxynaphthanlene derivative **7**[36] with the tosylate **6** in the presence of K_2CO_3 and 18-crown-6 as a phase-transfer catalyst afforded compound **9** in 79% yield. A subsequent hydrogenolysis of **8** gave the dioxynaphthalene derivative **8** in 78% yield. Another etherification of the naphthol derivative **9** with the TTF-monotosylate **10**[7g] under the same conditions provided the alcohol **11** in 60% yield, which was then tosylated to obtain compound **12** in 84% yield. Compound **12** was etherified with 2,6-diisopropyl-4-hydroxymethyl phenol **13** to furnish the dumbbell-shaped compound **14** in 80% yield. Finally, a macrocyclization of **15**·2PF$_6$ with α,α′-dibromo-*p*-xylene, templated by **14**, followed by a counteranion exchange with NH_4PF_6 afforded the bistable [2]rotaxane **4**·4PF$_6$ in 45% yield. The benzyl alcohol functionality at the TTF end of the [2]rotaxane **4**·4PF$_6$ is available for its further derivatization.

Syntheses of [2]Rotaxane 1·4PF$_6$ and Tetrad 2. The synthesis of the multicomponent rotaxane **1**$^{4+}$ is illustrated in Scheme 2. The P−C$_{60}$ dyad **3**,[23] containing a reactive carboxylic acid group, was esterified with the rotaxane **4**·4PF$_6$ using 2-chloro-4,6-dimethoxy-1,3,5-triazine, 4-methylmorpholine, and dimethyl-4-aminopyridine (DMAP) as the activating agents to afford the title rotaxane **1**$^{4+}$ in 90% yield. Similarly, an esterification of the dyad **3**[23] with the alcohol **11** using the same conditions furnished the tetrad **2** in a near quantitative yield as described in Scheme 3.

UV−vis−NIR Spectroscopy. The [2]rotaxane **1**$^{4+}$ is a multicomponent species, which contains a large number of chromophoric units (Figures 1 and 2). Its absorption spectrum in DMF solution (Figure 3) shows multiple peaks throughout

(38) (a) Anelli, P.-L., et al. *J. Am. Chem. Soc.* **1992**, *114*, 193−218. (b) Ashton, P. R.; Brown, G. R.; Isaacs, N. S.; Giuffrida, D.; Kohnke, F. H.; Mathias, J. P.; Slawin, A. M. Z.; Smith, D. R.; Stoddart, J. F.; Williams, D. J. *J. Am. Chem. Soc.* **1992**, *114*, 6330−6353. (c) Asakawa, M.; Ashton, P. P.; Ballardini, R.; Balzani, V.; Belohradsky, M.; Gandolfi, M. T.; Kocian, O.; Prodi, L.; Raymo, F. M.; Stoddart, J. F.; Venturi, M. *J. Am. Chem. Soc.* **1997**, *119*, 302−310.

Scheme 2. Synthesis of the Multicomponent [2]Rotaxane **1**·4PF_6

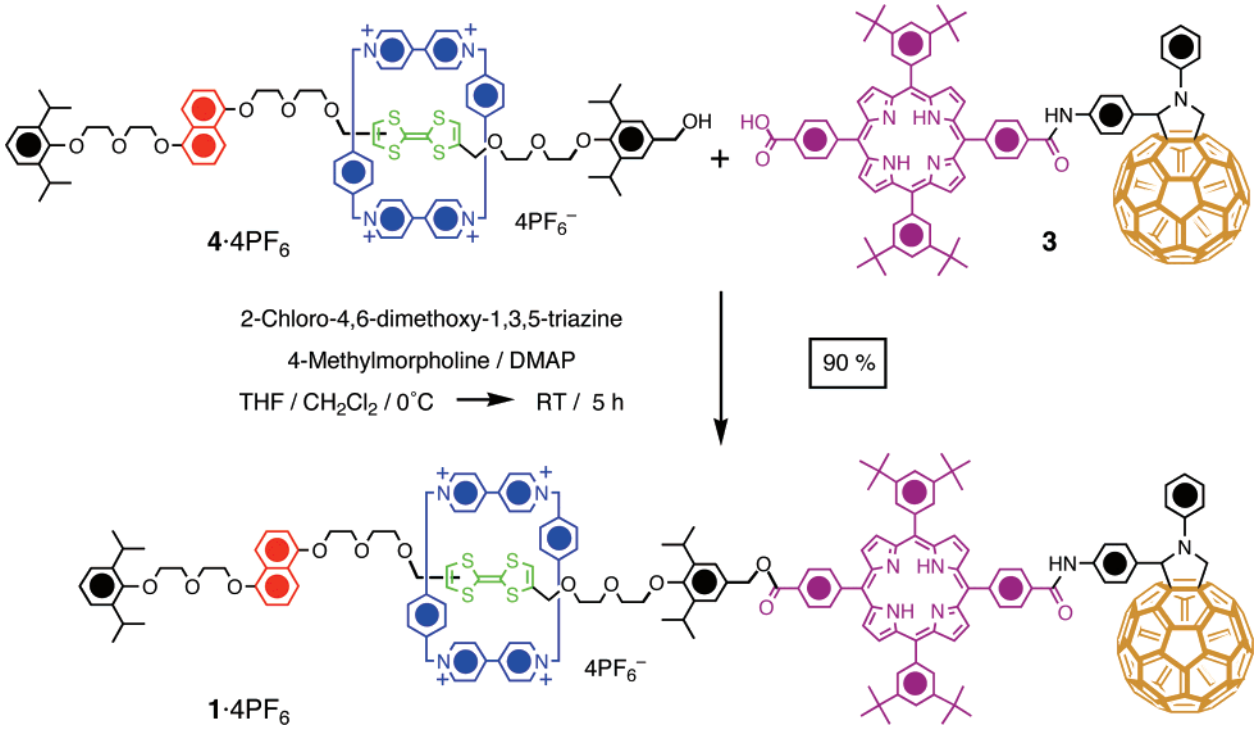

Scheme 3. Synthesis of the Tetrad **2**

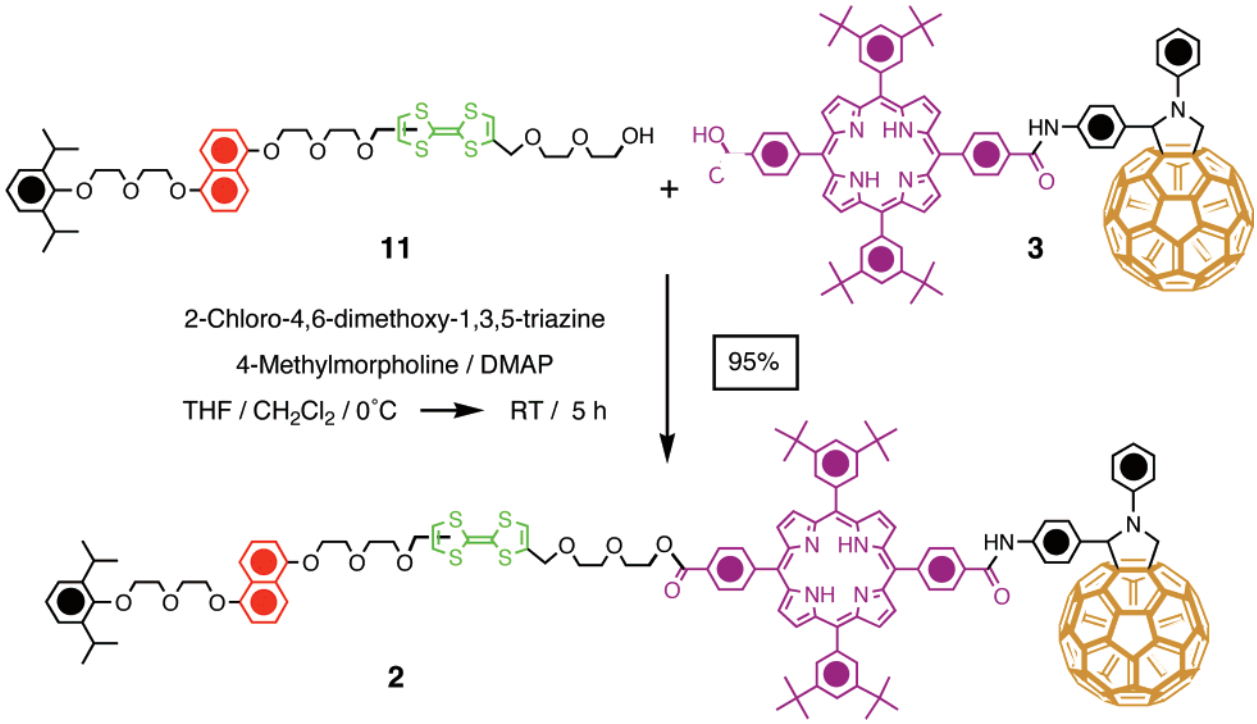

the near UV and visible regions and a broad and weak band centered around 840 nm, which extends into the near-infrared. The absorption features in the UV−vis region can be attributed to the corresponding chromophoric units—namely, C_{60}, porphyrin, TTF, DNP, and 4,4′-bipyridinium dication—by comparison with model compounds.[39] Specifically, the band peaking at 267 nm is ascribed to C_{60} and the 4,4′-bipyridinium units of $CBPQT^{4+}$; the broad absorption between 300 and 400 nm is assigned to the C_{60}, TTF, and DNP units; the sharp band at $\lambda_{max} = 419$ nm is the porphyrin Soret band; and the features from 500 through 650 nm are attributed to the porphyrin Q bands.[30] The broad band at 840 nm (Figure 3b) is characteristic[31] of a CT interaction between the electron-rich TTF component and the electron-deficient $CBPQT^{4+}$ ring.

(39) For solubility reasons, it was not possible to obtain the absorption spectra of all the compounds shown in Figure 2 in the same solvent. Hence, the spectra of rotaxanes $\mathbf{1}^{4+}$ and $\mathbf{4}^{4+}$ were measured in DMF and the spectra of all other compounds, except $CBPQT^{4+}$, were measured in THF. The spectrum of $CBPQT^{4+}$ was recorded in MeCN because its absorption bands fall in a spectral region below the cutoff wavelength of DMF.

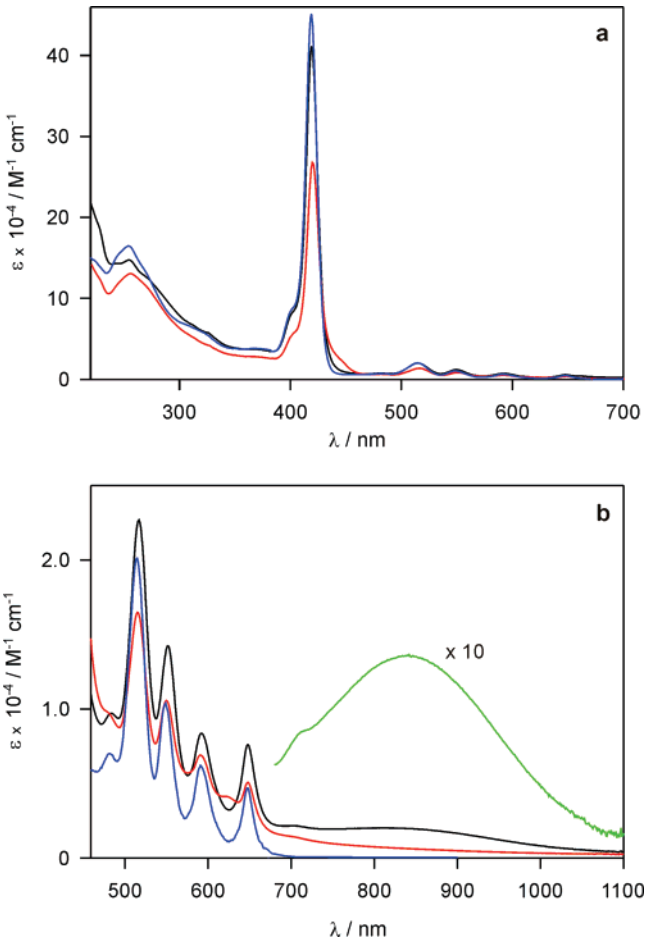

Figure 3. (a) UV−visible absorption spectrum of $\mathbf{1}^{4+}$ in DMF (black trace), sum of the spectra of its separated molecular components, **2** in THF and $CBPQT^{4+}$ in MeCN (red trace), and sum of the spectra for compounds **18**, **19**, **20**, and **21** in THF and $CBPQT^{4+}$ in MeCN (blue trace) which serve as models for the chromophoric units contained in $\mathbf{1}^{4+}$. The spectrum of tetrad **2** in DMF is nearly identical to that in THF. (b) Detail of the visible−NIR region for the spectra described in part (a). The green trace shows the difference between the absorption spectrum of $\mathbf{1}^{4+}$ and that of **2** in the 700−1100 nm region.

A careful analysis of the absorption spectra of all the compounds examined (Figure 2) shows, however, that the absorption features of multicomponent species **2**, **3**, and **16** cannot be obtained simply by linear combinations of the bands of their chromophoric units. The absorption spectrum of dyad **3** is slightly different from the sum of the spectra of its components **20** and **21** (see Supporting Information). A decrease in the intensity of the porphyrin peaks and an increase of absorption at around 300 nm indicates the occurrence of electronic interactions between the C_{60} and P units in the ground state. It is more likely that such interactions occur through space—molecular models indicate that the two units can easily approach each other in a face-to-face fashion—rather than through bonds, because the linker between the units is not fully conjugated. The presence of through space electronic interactions in covalently linked P−C_{60} species is well documented for flexible systems,[40] whereas it is not observed in dyads with rigid bridges.[34,41]

The absorption bands of triad **16** (Figure 4) are noticeably perturbed compared to those of its constituents, taken as the dyad **3** and the TTF derivative **19**. The C_{60} absorption around 260 nm becomes less intense, the Soret band of the P unit is weaker and broader, and a weak tail is observed at $\lambda > 600$ nm. To our knowledge, there are no reports in the literature on ground-state electronic interactions in TTF−porphyrin systems,[42] while intramolecular donor−acceptor interactions in covalently linked TTF−C_{60} have been observed[43] to cause a decrease in the fullerene UV absorption and the appearance of a weak absorption tail at $\lambda > 600$ nm. In summary, our observations suggest that the ground state of the triad **16** is characterized by non-negligible through-space electronic interactions involving the electron-accepting C_{60} unit and the electron-donating P and TTF units.

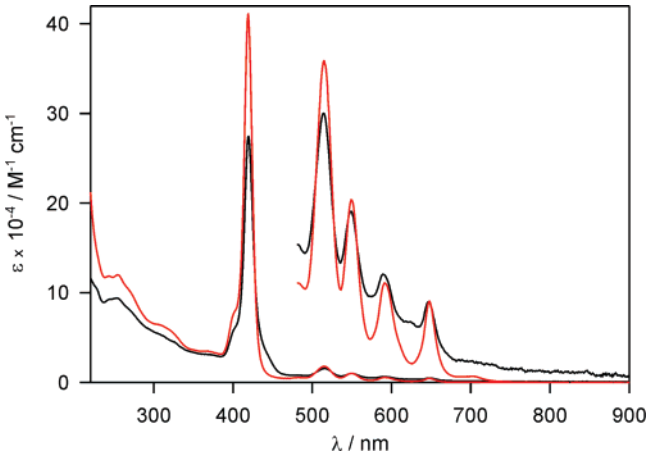

Figure 4. UV−visible absorption spectrum in THF of the triad **16** (black trace) and sum of the spectra of the dyad **3** and the TTF derivative **19** (red trace).

The absorption spectrum of the tetrad **2** is very similar to that of the parent triad **16** at wavelengths longer than 350 nm (see Supporting Information). The fact that the sharp absorption features of the DNP unit at $\lambda < 350$ nm are no longer observed in **2** indicates[25b,38a] that such a unit is also engaged in CT interactions with the other chromophoric components. Inspection of CPK molecular models indicates that the tetrad **2** is a very flexible molecule. Therefore, we reason that in solutions tetrad **2** occurs as folded conformations—akin to foldamers[44] which form folded secondary structures, stabilized by noncovalent interactions, namely, $\pi-\pi$-stacking, hydrogen bonding interactions, as well as solvophobic forces. In the triad **16** and tetrad **2** a preponderance of folded conformations are made possible by the presence of the flexible ethylene glycol linkers among the P, TTF, and DNP units which allow the molecules to fold up in such a way that the electron-donating (P, TTF, and DNP) and -accepting (C_{60}) units can interact with each other electronically (Figure 5) on account of favorable $\pi-\pi$-stacking interac-

(40) Armaroli, N.; Accorsi, G.; Song, F.; Palkar, A.; Echegoyen, L.; Bonifazi, D.; Diederich, F. *ChemPhysChem* **2005**, *6*, 732−743 and references therein.
(41) Lembo, A.; Tagliatesta, P.; Guldi, D. M. *J. Phys. Chem. A* **2006**, *110*, 11424−11434.
(42) Covalently linked TTF-porphyrin species: Sadaike, S.; Takimiya, K.; Aso, Y.; Otsubo, T. *Tetrahedron Lett.* **2003**, *44*, 161−165.
(43) Allard, E.; Cousseau, J.; Ordúna, J.; Garín, J.; Luo, H.; Araki, Y.; Ito, O. *Phys. Chem. Chem. Phys.* **2002**, *4*, 5944−5951.
(44) (a) Gellman, S. H. *Acc. Chem. Res.* **1998**, *31*, 173−180. (b) Hill, D. J.; Mio, M. J.; Prince, R. B.; Hughes, T.; Moore, J. S. *Chem. Rev.* **2001**, *101*, 3893−4011. (c) Schmitt, J.-L.; Stadler, A.-M.; Kyritsakas, N.; Lehn, J.-M. *Helv. Chim. Acta* **2003**, *86*, 1598−1624. (d) Kelley, R. F.; Rybtchinski, B.; Stone, M. T.; Moore, J. S.; Wasielewski, M. R. *J. Am. Chem. Soc.* **2007**, *129*, 4114−4115.

tions, a situation which is further supported by the electrochemical data (vide infra).

Interestingly, on going from the tetrad **2** to the multicomponent [2]rotaxane $\mathbf{1}^{4+}$ the absorption spectrum becomes much more similar to that obtained by summing up the spectra of the single chromophoric units (Figure 3). This change is most evident from the intensity recovery of the porphyrin absorption bands. Presumably, the presence of $CBPQT^{4+}$ around the TTF station prevents the occurrence of the intercomponent electronic interactions observed in tetrad **2**.

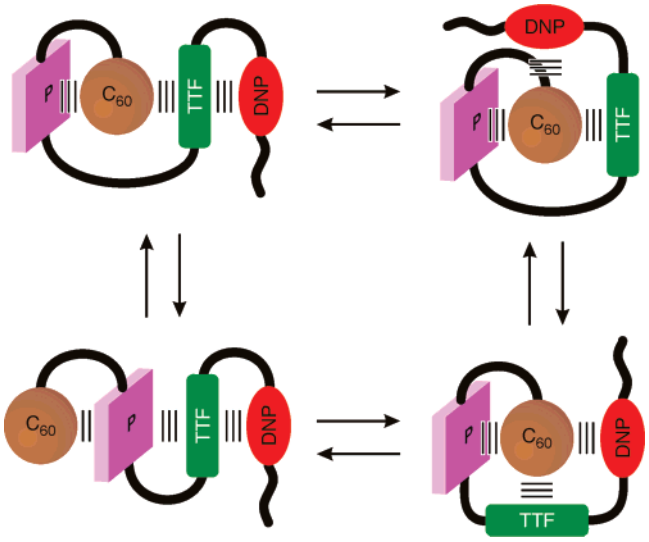

Figure 5. Schematic representation of the chemical equilibrium between four possible folded conformations for the tetrad **2** in THF solution, in which the electron-donating (P, TTF, and DNP) and -accepting (C_{60}) units can interact electronically with each other.

A quantitative comparison of the CT bands of $\mathbf{1}^{4+}$ and the model [2]rotaxane $\mathbf{4}^{4+}$ (Supporting Information) indicates that the $CBPQT^{4+}$ ring is engaged in CT interactions with the TTF station in about 75% of the $\mathbf{1}^{4+}$ molecules. This behavior could be caused by a competition between $CBPQT^{4+}$ and C_{60} electron acceptors for the electron-donating TTF unit. In such a case, it is to be expected that in 25% of the $\mathbf{1}^{4+}$ molecules the $CBPQT^{4+}$ surrounds the DNP station; however, this hypothesis cannot be confirmed because the weak DNP−$CBPQT^{4+}$ CT band (λ_{max} = 515 nm, ϵ = 650 M^{-1} cm^{-1} in MeCN)[25b] would be buried under the intense bands of the porphyrin chromophore and, therefore, undetectable.

Electrochemistry. The potentials for the redox processes observed in voltammetric experiments for the multicomponent rotaxane $\mathbf{1}^{4+}$, its dumbbell-shaped tetrad component **2**, and some model compounds (Figure 2) are listed in Table 1. These data are important for (i) applying suitable electrochemical stimuli to $\mathbf{1}^{4+}$ in order to trigger specific molecular movements and (ii) identifying the electron-transfer processes that can be expected to occur upon light absorption in the rotaxane and in its model compounds.

The cyclic voltammetric curve obtained for $\mathbf{1}^{4+}$ in DMF (Figure 6) shows as many as nine redox waves in the potential window examined, emphasizing once again the multicomponent nature of this rotaxane. Assignment of each redox wave to the corresponding electroactive unit is possible from a comparison with the behavior of appropriate reference species (Figure 2 and Table 1). Before discussing in detail the voltammetric behavior

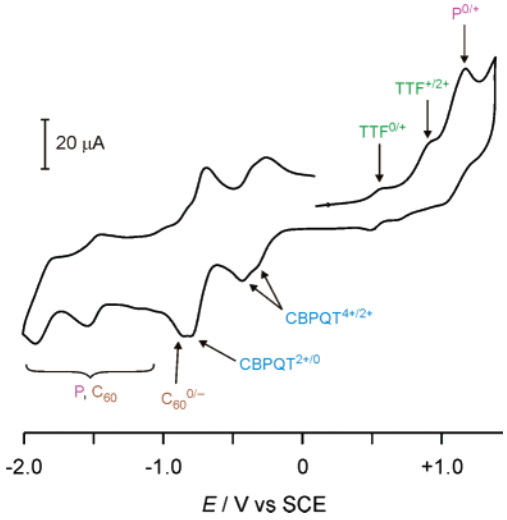

Figure 6. Cyclic voltammetry of $\mathbf{1}^{4+}$ in DMF (1.0×10^{-3} M, 0.1 M $TBAPF_6$) recorded at 200 mV s^{-1} with each of the peaks assigned to a particular electroactive unit of the rotaxane.

of $\mathbf{1}^{4+}$, it is necessary to describe the results obtained for the molecular components and some model compounds.

The electrochemical behaviors of the tetrad **2** and its model constituents, namely, TTF (**19**), the porphyrin **20**, the fullerene **21**, the dyad **3**, and the triad **16**, were investigated in THF (Table 1). The redox processes recorded for the dyad **3** fall at potential values expected[23b,45,46] for its porphyrin and C_{60} moieties. This observation indicates that the electronic interactions between such units in the dyad, which are revealed from the spectroscopic data, have a negligible effect on the redox potentials. For the triad **16** the oxidation of the porphyrin unit cannot be observed within the potential window explored and, therefore, occurs most likely at potentials higher than +1.4 V vs SCE. Moreover, the processes for the TTF oxidation (+0.53 and +0.80 V) are positively shifted compared to the same processes in model compound **19** (+0.42 and +0.71 V) and exhibit electrochemical irreversibility as well as a current intensity ca. 30% weaker than that expected for monoelectronic processes (Supporting Information). These observations are in agreement with the UV−vis spectroscopic data and suggest that the porphyrin and TTF units of **16** are involved in intramolecular electronic interactions in which they presumably act as electron donors and, as a consequence, become more difficult to oxidize. The lack of electrochemical reversibility and the decrease in the current intensity for TTF oxidation could be explained by the presence of folded conformations in which such a unit is shielded and cannot approach the electrode surface.[47] This hypothesis is consistent with the fact that the electrochemical reversibility and current intensity of the TTF oxidation processes increase by adding 15% of MeCN to the THF solution (see Supporting Information) in order to improve solvation. The electron-accepting counterpart is expected to be the fullerene unit; however, little or no change in the potential values for reduction of the C_{60} moiety is observed compared (Table 1) to the dyad

(45) (a) Carano, M.; Da Ros, T.; Fanti, M.; Kordatos, K.; Marcaccio, M.; Paolucci, F.; Prato, M.; Roffia, S.; Zerbetto, F. *J. Am. Chem. Soc.* **2003**, *125*, 7139−7144. (b) Sandanayaka, A. S. D.; Araki, Y.; Ito, O.; Deviprasad, G. R.; Smith, P. M.; Rogers, L. M.; Zandler, M. E.; D'Souza, F. *Chem. Phys.* **2006**, *325*, 452−460.

(46) Kadish, K. M.; Royal, G.; van Caemelbecke, E.; Gueletti, L. In *The Porphyrin Handbook*; Kadish, K. M., Smith, K. M., Guilard, R., Eds.; Academic Press: San Diego, 2000; Vol. 9, pp 1−219.

Table 1. Reduction Potential Values (in V vs SCE) for the Compounds Examined[a]

compound (solvent)[b]	assignment											
	$DNP^{+/0}$	$P^{+/0}$	$TTF^{2+/+}$	$TTF^{+/0}$	$CBPQT^{4+/3+}$	$CBPQT^{3+/2+}$	$CBPQT^{2+/0}$	$C_{60}{}^{0/-1}$	$C_{60}{}^{-1/-2}$	$P^{0/-1}$	$P^{-1/-2}$	$C_{60}{}^{-2/-3}$
rot. $\mathbf{1}^{4+}$ (DMF)	+1.37[c]	+1.11[c]	+0.91[c,d]	+0.51[c,d]	−0.28	−0.39	−0.73[e]	−0.84	−0.99	−1.39[c]	−1.48	−1.82
tetrad **2** (THF)	+1.23	+1.35[c]	+0.75[c,d]	+0.46[c,d]				−0.50	−1.05[c]	−1.71[c]		*f*
triad **16** (THF)		*f*	+0.80[c,d]	+0.53[c,d]				−0.51	−1.07	−1.23	−1.55	*f*
dyad **3** (THF)		+1.34[c]						−0.53	−1.07	−1.26	−1.56	−1.78
porphyrin **20** (THF)		+1.31[c]								−1.23	−1.56	
fullerene **21** (THF)								−0.53	−1.20[c]			−1.82[c]
TTF **19** (THF)			+0.71	+0.42								
rot. $\mathbf{4}^{4+}$ (DMF)	*f*		+0.74	+0.55	−0.29	−0.36	−0.73[e]					
$CBPQT^{4+}$ (DMF)					−0.23[e]		−0.67[e]					
dumbbell **17** (DMF)	+1.34[c]		+0.72	+0.46								

[a] Halfwave potential values referring to reversible and monoelectronic processes, unless otherwise noted. [b] For solubility reasons, it was not possible to perform the electrochemical experiments for all the compounds shown in Figure 2 in the same solvent. Hence, the experiments for compounds $\mathbf{1}^{4+}$, $\mathbf{4}^{4+}$, and $CBPQT^{4+}$ were carried out in DMF, and those of all other compounds were carried out in THF. In all cases 0.1 M tetrabutylammonium hexafluorophosphate was the supporting electrolyte. [c] Irreversible or poorly reversible process; potential estimated from the DPV peak. [d] The intensity of the CV wave is much weaker than that expected for a monoelectronic process. [e] Bielectronic process. [f] Not observed.

3. It is possible that these processes are not much affected by through-space electronic interactions involving the C_{60} moiety owing to the strong delocalization of the additional electrons in the reduced fullerene unit.

The CV profile for the tetrad **2** is similar to that of the triad **16**, although a comparison of the redox potentials indicates weaker intercomponent interactions compared to those in the triad. The current intensities associated with the TTF oxidations are again considerably weaker than those expected for monoelectronic processes, suggesting the presence of folded conformations (Figure 5) which in this case are not affected by the addition of up to 20% MeCN to the THF solution.

The voltammetric data obtained in DMF for the rotaxane $\mathbf{4}^{4+}$—which is a model for the mechanical switching part of $\mathbf{1}^{4+}$—the dumbbell-shaped component **17**, and the $CBPQT^{4+}$ ring are also gathered in Table 1 (cyclic voltammograms are reported as Supporting Information). $CBPQT^{4+}$ exhibits the usual two reversible bielectronic reduction processes (−0.23 and −0.67 V) assigned to the consecutive one-electron reductions of the two equivalent bipyridinium units, both slightly shifted to more negative potentials compared to those observed in MeCN.[38a] No oxidation process is detected. Compound **17** shows the two reversible monoelectronic oxidation processes of the electron-rich TTF unit, generating the TTF^{+} and TTF^{2+} species, respectively, and, at more positive potentials, the irreversible oxidation of the DNP unit. No reduction process is observed.

In the rotaxane $\mathbf{4}^{4+}$ the first two reduction processes (−0.29 and −0.36 V vs SCE, Table 1) are assigned to the reversible one-electron reduction of each of the two bipyridinium units present in the $CBPQT^{4+}$ ring. These potential values are more negative than the corresponding first (two-electron) process, measured for $CBPQT^{4+}$ alone because of the CT interaction with the TTF unit. The small albeit detectable splitting of the $CBPQT^{4+/2+}$ reduction into two monoelectronic waves shows that, in $\mathbf{4}^{4+}$, the two bipyridinium units of the ring, which are expected to be topologically equivalent, are not electrochemically equivalent. Such an effect was previously observed in related rotaxanes and attributed[7g,17d,48] to the fact that the $CBPQT^{4+}$ ring, while encircling a given electron-donating station, is involved in alongside interactions with the other electron-rich units. Such a behavior implies the presence of folded conformations wherein the two bipyridinium sides of the ring experience chemically different environments. The bielectronic process observed at −0.73 V is assigned to the reduction of $CBPQT^{2+}$ to its neutral form ($CBPQT^{0}$). The fact that this process is also negatively shifted compared to the same process in the free cyclophane indicates that $CBPQT^{2+}$ is still involved in electronic interactions with the dumbbell-shaped component. The bielectronic nature of the process indicates that, in the doubly reduced $\mathbf{4}^{2+}$ rotaxane, the two bipyridinium units of the ring gain topological equivalence.

Considering only the region of positive potentials, the first oxidation process of the TTF unit is anodically shifted (+90 mV) compared to the same process in **17**, whereas the second TTF oxidation occurs at a very similar potential. This behavior indicates that (i) the $CBPQT^{4+}$ ring is located initially on the

(47) The hindrance of electron-transfer processes for redox sites deeply enclosed within a molecular structure, e.g., in dendrimers, is a well-documented phenomenon. For example, see: (a) Cardona, C. M.; Mendoza, S.; Kaifer, A. E. *Chem. Soc. Rev.* **2000**, *29*, 37−42. (b) Gorman, C. B.; Smith, J. C. *Acc. Chem. Res.* **2001**, *34*, 60−71. (c) Hong, Y. R.; Gorman, C. B. *Langmuir* **2006**, *22*, 10506−10509. The lack of expected redox processes has also been observed in dendrimers containing multiple electroactive units both in the core and in the periphery and was attributed to the presence of conformations in which some of the redox sites are not accessible. See: (d) Baker, W. S.; Lemon, B. I., III; Crooks, R. M. *J. Phys. Chem. B* **2001**, *105*, 8885−8894. (e) Marchioni, F.; Venturi, M; Ceroni, P.; Balzani, V.; Belohradsky, M.; Elizarov, A. M.; Tseng, H.-R.; Stoddart, J. F. *Chem.—Eur. J.* **2004**, *10*, 6361−6368.

(48) Yamamoto, T.; Tseng, H.-R.; Stoddart, J. F.; Balzani, V.; Credi, A.; Marchioni, F.; Venturi, M. *Collect. Czech. Chem. Commun.* **2003**, *68*, 1488−1514.

TTF station and (ii) after the first oxidation of this unit the ring moves away, leaving the second oxidation process unaltered compared to that in the dumbbell-shaped component. The oxidation of the DNP unit is not observed within the potential window examined, most likely because this process falls at potentials higher than +1.5 V vs SCE on account of the fact that it becomes surrounded by the $CBPQT^{4+}$ ring after the oxidation of the TTF station. This hypothesis is in fact confirmed by spectroelectrochemical experiments (see Supporting Information).

In the multicomponent rotaxane $\mathbf{1}^{4+}$ the first three reduction processes are very similar to those of $\mathbf{4}^{4+}$ and are assigned to the $CBPQT^{4+}$ component. The splitting of the $CBPQT^{4+/2+}$ reduction into two monoelectronic waves (110 mV) is more evident than that in $\mathbf{4}^{4+}$ (70 mV) and shows that also $\mathbf{1}^{4+}$ exists as folded conformations[7g,17d,48] in which the electrochemical equivalence of the two bipyridinium units of the ring is lost. The third process, observed at −0.73 V, is bielectronic and therefore assigned to the $CBPQT^{2+/0}$ reduction. The successive process at −0.84 V is assigned[45] to the first monoelectronic reduction of the electron-accepting C_{60} unit, whereas the following four processes that are observed through the region from −0.9 to −1.9 V are attributed[23b,45,46] to reductions involving the C_{60} and porphyrin units (Table 1).

On the oxidation side, the two poorly reversible processes at +0.51 and +0.91 V vs SCE are assigned to the two monoelectronic oxidations of the TTF unit. The first one occurs at a potential similar to that found for the corresponding process in $\mathbf{4}^{4+}$, whereas the second TTF-centered oxidation is considerably more difficult in $\mathbf{1}^{4+}$ than in $\mathbf{4}^{4+}$. This observation may suggest that the $CBPQT^{4+}$ ring is still encircling the mono-oxidized TTF station but would also be consistent with a stabilization of the TTF^{+} species and/or destabilization of the TTF^{2+} species, no longer surrounded by the ring, because of electronic interactions with the other units present in the rotaxane structure. Spectroelectrochemical data (vide infra) are also in good agreement with this latter interpretation. Two further irreversible oxidation processes observed at +1.11 and +1.37 V are attributed to the porphyrin[23b,46] and DNP[14,17d−g] units, respectively.

It is important to note that the current intensity associated with the TTF oxidation processes in $\mathbf{1}^{4+}$ is considerably weaker than that expected for one-electron processes. A lack of current intensity in the TTF oxidation waves is observed also for the triad **16** and the tetrad **2** in THF. This issue is an important one because the shuttling operation of $\mathbf{1}^{4+}$ relies on the reversible oxidation of its TTF unit. The UV−vis experiments suggest that in $\mathbf{1}^{4+}$ the intercomponent interactions involving the TTF, P, and C_{60} moieties, observed for **16** and **2**, are impeded by the presence of the $CBPQT^{4+}$ ring encircling the TTF unit. The reduction behavior of the $CBPQT^{4+}$ ring shows, on the other hand, that the molecules of $\mathbf{1}^{4+}$ (and $\mathbf{4}^{4+}$) occur as folded conformations. Nevertheless, the current intensities for the TTF oxidations in $\mathbf{4}^{4+}$ are as expected for monoelectronic processes. Taken together, these observations indicate that the shielding of the TTF unit toward electrochemical oxidation is a nontrivial behavior of the rotaxane $\mathbf{1}^{4+}$ and has to be related to its complex multicomponent structure.

Spectroelectrochemistry. The complex voltammetric behaviors of the multicomponent [2]rotaxane $\mathbf{1}^{4+}$, as well as the corresponding tetrad **2**, particularly as far as the oxidations of the TTF unit are concerned, provided the motivation to undertake spectroelectrochemical investigations. In the present studies, the isolation of the intense Soret band (λ_{max} = 419 nm, ϵ = 410 000 M^{-1} cm^{-1}) allows us to monitor the co-conformational changes within the molecule in response to redox stimulation by visualizing the diagnostic, albeit weaker, absorption features in the 475−900 nm spectroscopic window, such as (a) the TTF^{+} absorption peak at 600 nm, (ii) the TTF → $CBPQT^{4+}$ CT band at 840 nm, and (iii) the $CBPQT^{2+}$ absorption peak at 600 nm.[31] The differential absorption spectra (ΔA) were derived from the original spectra recorded during electrolysis in an attempt to distinguish the appearance and disappearance of certain peaks from the overlapping Q-bands of the porphyrin chromophore in the 450−650 nm region. Spectroelectrochemical results for the TTF model **19** and the rotaxane $\mathbf{4}^{4+}$ can be found in the Supporting Information.

The spectroelectrochemical behavior of the tetrad **2** was investigated in DMF solution (Figure 7). The straight line passing through zero in Figure 7b represents the initial differential spectrum of the tetrad **2**. The onset of the TTF^{+} radical cation's absorption was first observed at E_{ap} = +0.45 V (vs Ag pseudoreference electrode), a situation which is consistent with the first oxidation potential of the TTF unit. The TTF^{+} radical cation's absorption bands continued to grow and ultimately reached their maximum (Figure 7, green trace) at E_{ap} = +0.60 V. The absorption features (green trace) of the

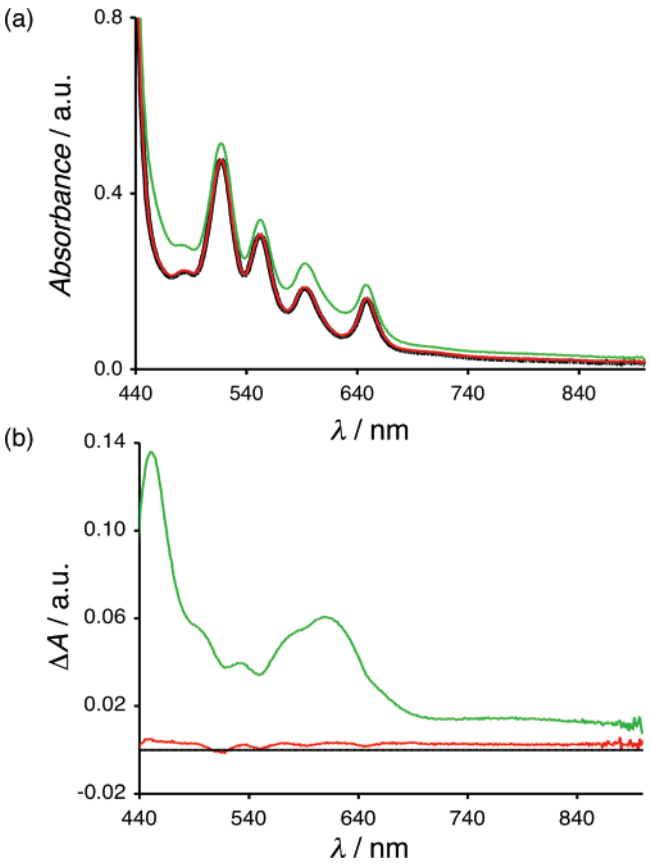

Figure 7. UV−visible spectroelectrochemical changes for the oxidation of tetrad **2** (1 mM DMF, 0.1 M $TBAPF_6$, optical path length 1 mm). (a) Absorption spectra; (b) differential absorption spectra (ΔA). Black traces, original spectra; green traces, spectra obtained after oxidation of the TTF unit to the TTF^{+} form at an applied potential of +0.60 V; red traces, spectra obtained after regeneration of the neutral TTF unit at an applied potential of −0.10 V.

oxidized form are similar but not identical to those of the TTF^{+} radical cation (Supporting Information) generated in the TTF-diol **19**. On the basis of the absorption coefficients for the TTF^{+} species at 600 nm one can estimate, however, that about 15% of the TTF units have been oxidized. Subsequently, reducing the TTF^{+} radical cation back to the neutral TTF ($E_{ap} = -0.10$ V) reproduced (Figure 7, red trace) the original spectrum. Thus, the electrochemical response of the tetrad **2** in DMF is reversible upon first one-electron oxidation of the TTF unit that, however, can be achieved only for a modest fraction of the tetrad molecules. These observations help to identify the spectroscopic changes that are indicative of the oxidatively induced switching process in the more complicated [2]rotaxane $\mathbf{1}^{4+}$.

We first investigated the oxidation of $\mathbf{1}^{4+}$ in DMF by applying a positive potential. The onset of spectroscopic changes (Figure 8) is observed when the applied potential is increased to +0.85 V (relative to a Ag pseudo-reference electrode). The characteristic absorption band of the TTF^{+} species, centered at 600 nm, emerges (Figure 8) over a period of 25 min at a constant applied potential (+0.85 V). On the basis of the absorption coefficients for the TTF^{+} species at 600 nm one can estimate, however, that ca. 30% of the TTF units have been oxidized. This change is concomitant with a decrease of the characteristic TTF → $CBPQT^{4+}$ CT band at 840 nm until complete disappearance (Figure 8), defining together an isosbestic point at 660 nm. These changes are similar but not identical to those recorded for the control rotaxane $\mathbf{4}^{4+}$, for which full monoelectronic oxidation of the TTF unit and complete disappearance of the CT band at 830 nm are observed (see Supporting Information). On the other hand, the absorption bands for the TTF^{+} species

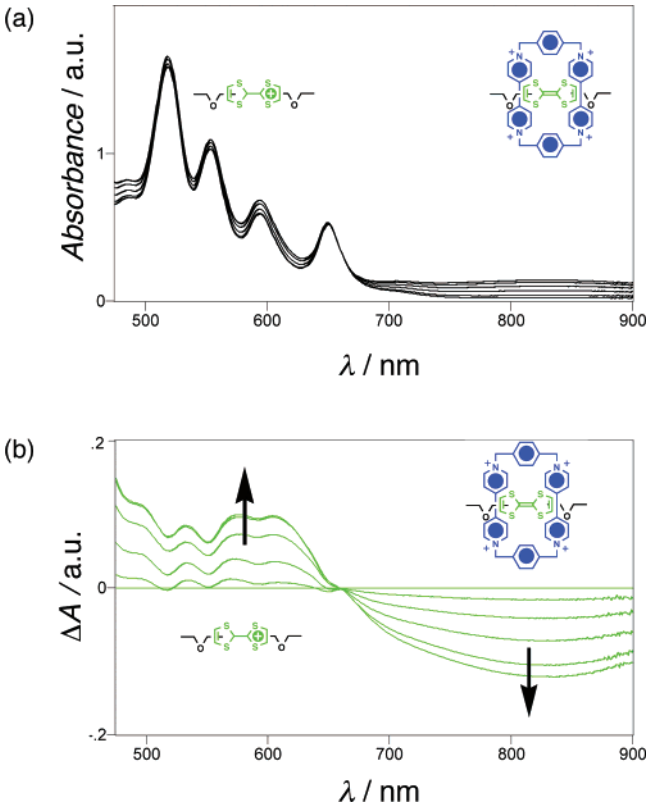

Figure 8. UV−visible spectroelectrochemical changes for the oxidation of $\mathbf{1}^{4+}$ (1 mM DMF, 0.1 M $TBAPF_6$, optical path length 1 mm) recorded over a period of 25 min at an applied potential of +0.85 V. (a) Absorption spectra; (b) differential absorption spectra (ΔA).

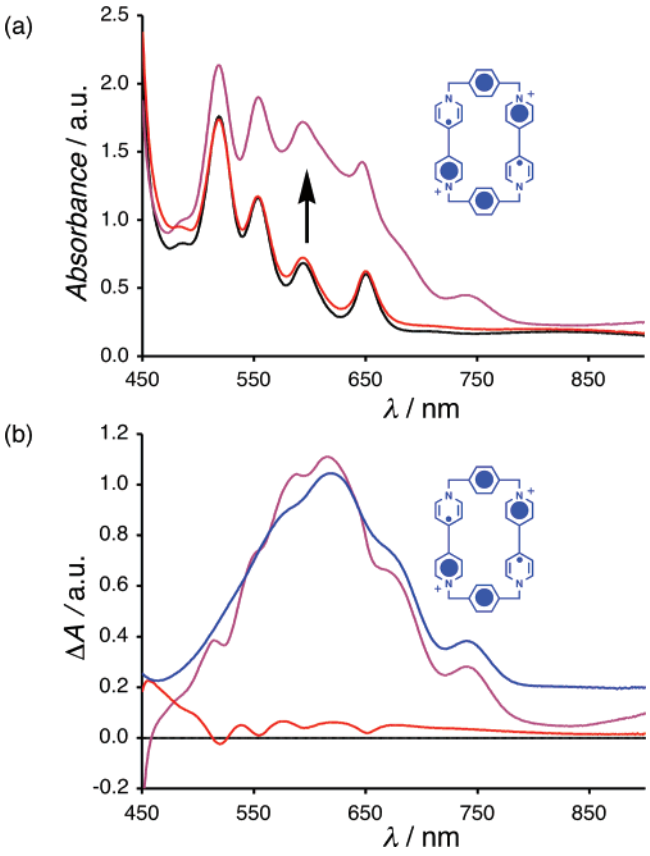

Figure 9. UV−visible spectroelectrochemical changes for the reduction of the $CBPQT^{4+}$ ring of $\mathbf{1}^{4+}$ (1 mM DMF, 0.1 M $TBAPF_6$, optical path length 1 mm). (a) Absorption spectra; (b) differential absorption spectra (ΔA). Black traces, original spectra; purple traces, spectra obtained after complete reduction of the $CBPQT^{4+}$ ring to the $CBPQT^{2+}$ form upon application of a potential from −0.25 to −0.40 V; red traces, spectra obtained after regeneration of the $CBPQT^{4+}$ ring at an applied potential of 0 V for $\mathbf{1}^{4+}$. The blue trace in panel b shows the absorption features of the $CBPQT^{2+}$ ring obtained upon electrochemical reduction of the [2]rotaxane $\mathbf{4}^{4+}$ in DMF under the same conditions employed for $\mathbf{1}^{4+}$.

are very similar to those obtained upon electrolysis of tetrad **2** (Figure 7). Had the ring remained encircling the TTF^{+} component, the 600-nm band would have been significantly affected.[49] The above observations on $\mathbf{1}^{4+}$ are consistent with a TTF unit encircled by a $CBPQT^{4+}$ ring (the major oxidative peak in related simpler rotaxanes is observed[14g,31] at around +0.8 V) and with the movement of the tetracationic $CBPQT^{4+}$ ring away from the singly oxidized TTF^{+} unit. Based on our extensive studies on simpler TTF−DNP-based bistable rotaxanes[14,17d−g,31,32] and the results gathered for $\mathbf{4}^{4+}$, we believe that electrochemical one-electron oxidation of the TTF unit in $\mathbf{1}^{4+}$ causes the displacement of the $CBPQT^{4+}$ ring onto the now-better electron-donating DNP station. Conclusive proof of the position of the tetracationic cyclophane, at this point, would have been the emergence of a characteristic weak DNP → $CBPQT^{4+}$ CT band at ca. 500 nm.[25b,31c] Unfortunately, we were unable to identify any increase in absorbance over and above the very intense porphyrin absorption peaks in this wavelength region.

The successive application of a potential of 0 V causes the disappearance of the TTF^{+} component's absorption peak at 600

(49) Nygaard, S.; Laursen, B. W.; Flood, A. H.; Hansen, C. N.; Jeppesen, J. O.; Stoddart, J. F. *Chem. Commun.* **2006**, 144−146.

nm, suggesting that reduction of the TTF^+ species back to the neutral TTF has occurred. However, the original spectrum of $\mathbf{1}^{4+}$ in the 475−700 nm region is not fully recovered, indicating that some decomposition takes place on the time scale of electrolysis (minutes) upon oxidation/reduction of the TTF station in the rotaxane. The decrease of the band at 600 nm is accompanied by a recovery of the TTF → $CBPQT^{4+}$ CT band at 840 nm to 75% of its original intensity. Kinetic effects can be ruled out because the intensity of this band does not increase with time.

To summarize, the spectroelectrochemical data confirm that the electrochemical oxidation of the TTF moiety in $\mathbf{1}^{4+}$ is hampered, possibly because of the presence of folded conformations in which this moiety cannot reach the electrode surface.[47] However, electrolytic oxidation of the TTF station can be partially achieved, causing the displacement of the $CBPQT^{4+}$ ring away from the TTF^+ species. Subsequent electrolysis at 0 V regenerates the neutral TTF unit, but only 75% of the $CBPQT^{4+}$ rings return to encircle it, as shown by the incomplete recovery of the CT band at 840 nm.

In principle, the movement of the $CBPQT^{4+}$ ring away from the TTF station could be achieved also by monoelectronic reduction of both its bipyridinium moieties to give the $CBPQT^{2+}$ form. This process is expected to destabilize the CT interactions with either the TTF or DNP donor units, thereby leaving the ring to move "freely" along the dumbbell, i.e., without being locked at either station. In order to explore this possibility we performed spectroelectrochemical experiments on the reduction of $\mathbf{1}^{4+}$. At an applied potential of −0.40 V, a structured band centered at 600 nm (Figure 9), typical of monoreduced 4,4′-bipyridinium units,[50] appears. On the basis of the absorption coefficients for the bipyridinium radical cation at 600 nm one can estimate that more than 90% of the total bipyridinium units have been reduced. A clear decay of the TTF → $CBPQT^{4+}$ CT band at 840 nm could not be observed because of the absorption tail of the $CBPQT^{2+}$ component in the 750−900 nm region. Back electrolysis at 0 V causes the disappearance of the bands characteristic of the reduced bipyridinium units, and the original spectrum is restored.

Conclusions

By following a modular strategy, we have synthesized and characterized a multicomponent [2]rotaxane designed to perform as an autonomous molecular shuttle powered by light. UV−vis−NIR absorption spectroscopy, together with electrochemical and chemical oxidation, studies have been employed to investigate the redox-controlled shuttling of an electron-accepting ring between two competitive electron-donating stations. The experimental results show that remarkable electronic interactions between the various units located on the dumbbell-shaped component take place, suggesting the existence of folded structures in solution. The TTF unit can be electrochemically oxidized only in a limited fraction of the $\mathbf{1}^{4+}$ molecules. In these species, removal of one electron from the TTF unit causes the shuttling of the $CBPQT^{4+}$ ring away from this station. The lack of complete electrochemical oxidation of the TTF unit is observed also for the dumbbell-shaped component of $\mathbf{1}^{4+}$ and for a molecular triad comprising TTF, porphyrin, and C_{60} modules. Most likely, these systems occur as conformations in which the TTF unit is buried inside a complex equilibrium mixture of conformations and co-conformations and is therefore protected against oxidation performed by an electric potential applied *externally*. Such a behavior limits the efficiency for the operation of rotaxane $\mathbf{1}^{4+}$ as a redox-driven molecular shuttle. The possibility of achieving TTF oxidation by an electric potential generated *internally* through intramolecular photoinduced electron transfer is currently under investigation.

In general terms, our results indicate that as the structural complexity increases, the overall properties of the system cannot be easily rationalized solely on the basis of the type and sequence of the functional units incorporated in the molecular framework, that is, its "primary" structure. Although some aspects of the behavior of the investigated compounds are not fully understood, it seems that higher-level conformational and co-conformational effects, which are reminiscent of those related to the secondary and tertiary structure[44] of biomolecules, have to be taken into consideration. The comprehension of these effects constitutes a stimulating scientific problem and a necessary step for the design of novel artificial molecular devices and machines.

Acknowledgment. We thank Professor Vincenzo Balzani and Dr. Nicolle Moonen for valuable discussions, and Dr. Alberto Di Fabio for his help in some experiments. This research was supported in the U.S. by a National Science Foundation's (NSF) Nanoscale Interdisciplinary Research Team (NIRT ECS-0103559) fund, an Office of Naval Research (ONR Contract number N00014-00-1-0216) grant, an NSF Equipment Grant (CHE-9974928), and the Center for Cell Mimetic Space Exploration (CMISE) − a NASA University Research, Engineering and Technology Institute (URETI), the award number being NCC2-1364. In Italy, the research was supported by the EU Biomach project (NMP2-CT-2003-505487), Ministero dell'Università e della Ricerca (PRIN 2006034123), Regione Emilia-Romagna (NANOFABER), and Università di Bologna (Progetto strategico CompReNDe).

Supporting Information Available: Experimental section, synthetic procedures, additional spectroscopic, voltammetric, and spectroelectrochemical data, as well as complete refs 17a, 25b, and 38a. This material is available free of charge via the Internet at http://pubs.acs.org.

JA0724590

(50) Ballardini, R.; Credi, A.; Gandolfi, M. T.; Giansante, C.; Marconi, G.; Silvi, S.; Venturi, M. *Inorg. Chim. Acta* **2007**, *360*, 1072−1082.